FORTSCHRITTE DER PHYSIK

VOLUME 38 1990 NUMBER 1

Fortschr. Phys. 38 (1990) 1, 1—34

Introduction to Quark-Gluon Plasma

V. M. EMEL'YANOV, YU. P. NIKITIN (†), A. V. VANYASHIN

Moscow Physical Engineering Institute, Moscow, USSR

Abstract

Problems of formation, evolution and detection of quark-gluon plasma are reviewed to fill a gap between theory and experiment.

Contents

Introduction

In the QCD development two characteristic stages have existed in the last decade. The first is the study of "hard" processes. As is well known, the coupling constant α_s of strong interactions decreases with increasing squared transferred 4-momentum $|Q^2|$ because of the asymptotic freedom. For $|Q^2| \gg \Lambda^2_{\rm QCD}$ ($\Lambda_{\rm QCD} \sim 200$ MeV) the coupling constant $\alpha_s \ll 1$, and calculations can be made within QCD perturbation theory. Such calculations were carried out intensely in the 70-ies. The QCD predictions were brilliantly confirmed by observation of hadron jets with large transverse momenta.

But in the quantitative comparison with experimental data the clear predictions of QCD perturbation theory are lost in the maze of soft process phenomenology. The point is that the particles which are actually observed are not QCD quarks and gluons but hadrons resulting from soft processes of quark hadronization.

By early 80-ies the QCD properties had been realized quite well within perturbation theory. It was perfectly clear, however, that the perturbative QCD was far from exhausting the theory as a whole. Such exceedingly important properties of strong interactions as color charge confinement, breaking of chiral invariance and, in the end, observed hadron masses are due to nonperturbative fluctuations in QCD. The following three among the nonperturbative QCD methods have been most intensely developed since early 80-ies: 1) lattice technique; 2) sum rules; 3) quasi-classical (instanton) method. The results obtained using these methods are discussed in detail below. We would only like to mention here that they have a common prediction according to which the natural QCD vacuum state is appreciably distinct from the vacuum of perturbation theory. How does the QCD vacuum change its state with increasing $\alpha_s(Q^2)$ and to what effects can this change lead?

To be solved, these complicated problems should be essentially simplified. To simplify we will consider a macroscopical system of quarks and gluons which obeys the laws of thermodynamics. At high temperatures $T \gg \Lambda_{\rm QCD}$, the characteristic momentum transfer in the interaction appears to be fairly large, $Q^2 \sim T^2 \ll \Lambda^2_{\rm QCD}$, and the running coupling constant becomes small, $\alpha_s \sim 1/\ln(Q^2/\Lambda^2_{\rm QCD}) \ll 1$. Owing to the asymptotic freedom of QCD, such a system is thus a relativistic gas of rather weakly interacting quarks and gluons — the so-called quark gluon plasma (QGP). Similar reasoning can be extended to high QGP densities because the characteristic interparticle distances turn out to be small.

The concept of hot hadronic matter was developed in a pioneering papers [1—3], where the statistical and hydrodynamical methods were used to study the strongly interacting particle ensemble. The prediction of hadron — quark phase transition was made in [4]. The same ideas are used nowdays, but the knowledge of hot hadronic matter resulting from QCD is added. The phase transition is qualitatively predicted in QCD [5, 6] and confirmed by lattice calculations [7]. The hadron-QGP transition temperature T_c appears to be equal about to 200 MeV [7] and the QGP density to be 3—4 times higher than the usual nuclear matter density.

Since the expected temperatures $T \sim T_c \sim \Lambda_{\rm QCD}$ refer to the infrared QCD region, the majority of models of the microscopical QCD system are of phenomenological character. Some of these models are considered in Sec. 1. It is instructive to note that the model assumptions are responsible not only for the critical parameters T_c and n_c (the QGP

density) of a given phase transition but also for the type and number of phase transitions. We may thus hope that new detailed experimental data will appreciably reduce the number of acceptable phenomenological models. The defficiency of the purely phenomenological approach is an uncertainty in the correspondence between a given model and the real dynamics of strong interactions. In this respect, the attempts to calculate the QGP thermodynamic functions directly on the basis of the QCD Lagrangian are much more attractive. In recent years, such calculations have been successful. In particular, a numerical integration of the lattice type QCD systems proves the existence of first- and second-order phase transitions at temperatures $T \simeq 200$ MeV in theories with gauge groups $SU(3)$ and $SU(2)$. The problems connected with phase transitions in lattice gauge theories are also analyzed in Sec. 1 along with the results of phase transition studies by the QCD sum rule method at finite temperatures. Section 1 is devoted to modern computational methods applied to critical temperatures and densities of phase transitions.

The interest in finite-temperature and finite-density QCD was first stimulated by cosmological and astrophysical problems. Only in the times of Big Bang and also deep inside neutron stars could one imagine the existence of the conditions typical of phase transitions in nuclear matter. These questions are unfortunately beyond the scope of the present review, but interested readers may follow up in more detailed study of [8].

The interest in the thermodynamical aspects of QCD has increased recently because there appeared an experimental possibility to create extreme conditions for the existence of nuclear matter by way of selecting specific events in hadron collisions and particularly high-energy heavy ions. The exciting possibility of reproducing in laboratory the conditions imitating those existed in the Universe at first moments of the "creation of the world" has led to a rapid advance in new experimental programs for seeking processes the cognitive interest in which is beyond the scope of elementary particle physics. A successful practical realization of these programs will be not only of scientific but also of universal value. Above mentioned possibility of investigating nuclear matter under extreme conditions does not imply, however, that phase transition must necessarily take place in high-energy ion-ion (AA) interactions. The point is that it is not clear a priori whether or not a local thermodynamic equilibrium in QGP is established in AA collisions, i.e. whether it is possible to describe such a system within thermodynamic approach. Another important question is what energy density and temperature of QGP can be attained in available and future ion accelerators. These questions are dealt with in Sec. 2 within hydrodynamic approach to AA interactions. The basic conclusion of Sec. 2 is as follows. At early stages of hydrodynamic expansion of a hadron cluster (fireball) formed in collision of heavy ($A \gtrsim 50$) nuclei of energy $E_{\text{c.m.}} \gtrsim 10$ GeV/nucleon in the centre-of-mass system, local temperatures $T \gtrsim 200$ MeV and densities 3—4 times higher than the ordinary nuclear density can be attained. Under such conditions, the quark-gluon plasma may appear as a new phase of hadron matter.

In Section 3 we are considering experimental signals of hadron-QGP transition in AA interaction, which is a very important question. Experimental signals may include momentum spectra of direct leptons and photons, strange and charmed mesons and baryons, etc. The main difficulty encountered in identification of QGP signals is that the hadron background is typically quite noticeable. Furthermore, it is at present difficult to identify a certain signal which would reliably testify to QGP formation. The actual situation is that the existence of QGP in AA interactions at high energies can be identified only from several indirect experimental signals. Several discovered features of hadron collisions at high energies which are typical of QGP signals are also analyzed in Sec. 3. In the concluding section we briefly consider the perspectives of the physical programs searching for a new states of hadron matter.

When preparing the text of this review, the authors tried not to overload the presentation with numerous formulas and paid particular attention to the qualitative physical

picture of the phenomenon. For details we refer the reader to the literature cited. The theory, phenomenology and QGP-seeking experiments are at present a rapidly developing branch of atomic nucleus and elementary particle physics. These questions are discussed at periodic International Conference on ultrarelativistic ion-ion interactions whose proceedings contain much instructive information [9–12]. The QGP physics is also dealt with in the recent reviews [13–17] and in the collected papers [18–19].

The authors are greatful to B. A. Dolgoshein, S. A. Voloshin, M. I. Gorenshtein, G. M. Zinov'ev, O. A. Mogilevsky, A. I. Bochkarev, and M. E. Shaposhnikov for fruitful discussions which helped them to formulate some of the problems touched upon in this review.

1. Hadron-Quark-Gluon Plasma Transition

1.1. Two QCD problems

In QCD, two basic problems associated with the vacuum structure are known: color charge confinement and spontaneous breaking of chiral symmetry. The confinement means the absence of color objects in the spectrum of observed physical hadron states. The spontaneous breaking of chiral symmetry is essentially as follows. When the quark (and antiquark) mass is zero, their right and left components in the QCD Lagrangian split (they are not mixed in interaction with vector gluons). This must lead to parity degeneracy of the physical states of the theory, i.e. to a double number of the physical states, which is however not confirmed by experiment. The QCD vacuum is chirally asymmetric because there exists practically a massless (as compared with other hadrons) pion with an odd intrinsic parity. Thus, at zero temperatures and normal nuclear densities, the QCD vacuum possesses a confinement property and a broken chiral symmetry.

In this section we are concerned with the theoretical models which show that with increasing temperature and density the QCD vacuum loses the confinement property and restores its chiral invariance. There obviously exist some temperature and baryon density ranges within which the hadron matter is in the hadron gas and quark-gluon plasma states respectively. One of the principal goals of this section is to obtain a phase diagram for hadron matter in terms of the variables T and n_B (temperature and baryon density) and to determine the critical values T_c and n_c. We would like to draw the reader's attention to two facts. First, the phase transition is certainly the problem of strong coupling in the theory. Unfortunately, theoreticians cannot now suggest any consistent recipe for computations in the strong coupling region. Phenomenological, quasi-classical, and other approaches to the problem will therefore be fairly reasonable. The second circumstance is that in spite of distinct starting assumptions, these models give close T_c and n_c values, this "unanimity" hardly being accidental. In our opinion, it reflects the essence of the QCD theory.

1.2. The two-phase model

Consider a two-phase system of particles consisting of non-strange hadrons, u, d quarks (antiquarks), and gluons. The thermodynamic variables in the system are temperature T, baryon chemical potential μ and volume V. When describing the hadron phase (the same as the QGP phase), we disregard interaction (the gas approximation). The ground-state energy shift in quark-gluon plasma, as compared with the ground state of the hadron gas, is taken into account in this model by introduction of the phenomenological constant B which is used in the bag model [20]. For the sake of simplicity we consider only two limiting cases, $\mu = 0$ and $T = 0$.

If the chemical potential is zero ($\mu = 0$), then at low temperatures the system will be a pion gas by the assumption. The pressure of such a gas is determined by the formula for a relativistic gas of noninteracting massless bosons

$$p_H(T, \mu = 0) = \frac{\pi^2}{90} g_H T^4, \tag{1.1}$$

where, with an account of the three charge states of pions,

$$g_H = 3. \tag{1.2}$$

According to the equation of state $p = \varepsilon/3$, the energy density of this gas is given by

$$\varepsilon_H(T, \mu = 0) = \frac{\pi^2}{30} g_H T^4. \tag{1.3}$$

At high temperatures one expects the QGP formation, i.e. its appearance will be determined by the sum of relativistic gluon (bose) gas and quark (fermi) gas pressures

$$p_Q(T, \mu = 0) = \frac{\pi^2}{90} g_Q T^4 - B. \tag{1.4}$$

The vacuum pressure (negative) is taken into account by means of the parameter B, and the quantity

$$g_Q = \left(2 \cdot 8 + \frac{7}{8} \cdot 2 \cdot 2 \cdot 2 \cdot 3\right) = 37, \tag{1.5}$$

where the spin and color degrees of freedom of gluons and quarks (antiquarks) are taken nto account. The energy density in the QGP phase is accordingly equal to

$$\varepsilon_Q(T, \mu = 0) = \frac{\pi^2}{30} g_Q T^4 + B. \tag{1.6}$$

Then in statistical physics there usually holds the equilibrium condition for two phases (hadrons and QGP) which makes it possible to find the critical temperature

$$p_H(T = T_c, \mu = 0) = p_Q(T = T_c, \mu = 0). \tag{1.7}$$

From this formula we have the estimate for the critical temperature of a possible phase transition

$$T_c = \left(\frac{45}{17\pi^2} B\right)^{1/4} \simeq 0.72 B^{1/4}. \tag{1.8}$$

Comparison of the hadron masses calculated in the bag model with their experimental values gives the estimate [20] of the constant

$$B^{1/4} = (0.20 \pm 0.05)\ \text{GeV}, \qquad B \simeq 0.17\ \text{GeV/fm}^3.$$

From (1.8) we have in this case $T_c \simeq 140$ MeV. We are obviously dealing with the first-order phase transition because at the transition point the energy density changes in a jump $\varepsilon_Q(T_c, 0) - \varepsilon_H(T_c, 0) = 4B$. The critical energy density for QGP formation is given by

$$\varepsilon_c = \frac{3 g_H}{g_Q - g_H} B = \frac{9}{34} B = 0.045\ \text{GeV/fm}^3. \tag{1.9}$$

Correspondingly, for the energy density exceeding

$$\varepsilon = \varepsilon_c + 4B = 0.73 \text{ GeV/fm}^3 \tag{1.10}$$

the hadron matter is entirely in the QGP phase.

Figure 1 illustrates the behaviour of the equation of state in the given model ($\mu = 0$) in the parametric form $p = p(T)$, $\varepsilon = \varepsilon(T)$.

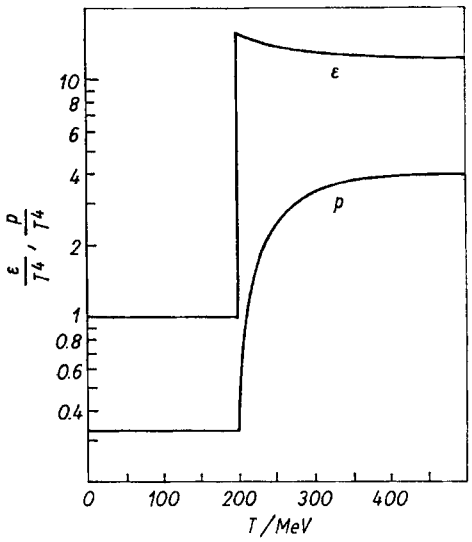

Fig. 1. Hadronic matter equation of state

Now proceed to another limiting case of the model — the zero temperature limit and a nonzero baryon chemical potential $\mu \equiv 3\mu_q$. Then in the hadron phase there exists a perfectly degenerate fermi-gas of baryons with pressure, energy density, and baryon density respectively equal to [21]

$$\begin{aligned} p_H(T = 0, \mu) &= \frac{1}{24\pi^2} \cdot 2 \cdot 2\mu_q{}^4; \\ \varepsilon_H(T = 0, \mu) &= \frac{1}{8\pi^2} \cdot 2 \cdot 2\mu_q{}^4; \\ n_B &= \frac{2}{3\pi^2} \mu_q{}^3. \end{aligned} \tag{1.11}$$

At high densities, the given system, as has already been mentioned, is in the QGP phase with pressure and energy density equal to

$$\begin{aligned} p_Q(T = 0, \mu) &= \frac{1}{24\pi^2} \cdot 4 \cdot 3 \cdot \mu_q{}^4 - B; \\ \varepsilon_Q(T = 0, \mu) &= \frac{1}{8\pi^2} \cdot 4 \cdot 3 \cdot \mu_q{}^4 + B. \end{aligned} \tag{1.12}$$

From the equilibrium condition $p_H(0, \mu_c) = p_Q(0, \mu_c)$ we find the critical value of the chemical potential

$$\mu_c = 3(3\pi^2 B)^{1/4} \simeq 7B^{1/4}. \tag{1.13}$$

The critical baryon density is in this case

$$n_c = 2(3\pi^2)^{-1/4} B^{3/4} \simeq 0.86 B^{3/4} \simeq 5 n_0, \tag{1.14}$$

where $n_0 = 0.17\,\mathrm{fm}^{-3}$ is the normal nuclear density. A more detailed investigation of the model for arbitrary temperatures and chemical potentials gives the phase diagram presented in Fig. 2.

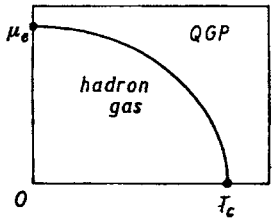

Fig. 2. Phase diagramm of hadronic matter

One can see from Fig. 2 that there are two experimental ways to form QGP: 1) by rising the hadron matter temperature or 2) by increasing baryon densities in AA interactions. The combination of both is most reasonable.

In this phenomenological phase transition model, the two-phase structure of a system of strongly interacting particles is introduced, in fact, ad hoc because in establishing the phase transition point the various analytical expressions for $p(T, \mu)$ are extrapolated into the region of intermediate temperatures and pressures. The shortage of this analysis is obvious: the procedure does not give evidence of the existence of phase transition, neither does it provide an insight into its nature. It automatically predicts a phase transition even in case it is actually absent, as in the well-known ionization problem [22]. The main task therefore is to give theoretical grounds to this phenomenological procedure. With this view we discuss several physical models which provide an insight into the nature and mechanisms of QGP-hadron phase transition.

1.3. Debye screening in QGP

It should be noted that the idea of phase transition, being a comparatively new one in nuclear physics and in elementary particle physics, is not at all new in solid state and molecular physics. And it would be unreasonable not to use the experience accumulated in these branches of physics in the study of phase transitions. For a qualitative understanding of the quark-gluon system behaviour predicted by QCD for densities $n \gg n_0$, consider qualitatively similar phase transitions in molecular physics.

Under normal pressure, hydrogen is insulator. A state with a nonzero electrical conductivity and with release of bound electrons may, however, appear at high densities [23]. This transition is caused by the fact that with increasing particle density in a system, the electric charge of a proton does not any longer have an effect upon the initially bound electron due to the screening produced by the charges of other protons and electrons of the system. The Debye radius of proton charge screening, λ_D, reaches atomic dimensions. The screening weakens the Coulomb interaction between proton and electron. The electrons become therefore quasi-free, and hydrogen is transformed into a metallic phase. The condition $\lambda_D = \lambda_B$ (λ_B is atomic radius) yields the parameters of insulator — metal phase transition.

Using similar reasonings, we estimate the critical temperature in QCD for the hadron matter (which is an "insulator" for color charges) to transform into a colour conductor —

a quark-gluon plasma. In the presence of other charges, the thermodynamic potential for a given charge g turns out to be equal to

$$\Omega_D = \frac{2\pi}{3} n\lambda_D^{-1}T^{-1}\frac{g^2}{4\pi}, \tag{1.15}$$

where T is temperature, n the total color charge density. The density of an ideal QGP in the QCD-interaction based on the gauge group $SU(3)$ is equal, according to [24, 25], to:

$$n = \frac{1.2}{\pi^2} g_Q T^3. \tag{1.16}$$

The expression for g_Q is given in formula (1.5). In first-order QCD perturbation theory, the QGP thermodynamic potential is

$$\Omega_D = \sqrt{\frac{\pi}{486}}\, 128\sqrt{2}\left(\frac{g^2}{4\pi}\right)^{3/2} T^3. \tag{1.17}$$

Comparing (1.15) and (1.17), we have

$$\lambda_D^{-1} = 1.81\left(\frac{g^2}{4\pi}\right)^{1/2} T. \tag{1.18}$$

The effective color charge g is connected with temperature by the relation that follows from the QCD predictions for a "running" constant of strong interaction

$$g^2/4\pi = 6\pi/29 \ln (4T/\Lambda_T), \tag{1.19}$$

where $\Lambda_T = 100$ MeV.

Putting the parameter λ_D equal to the typical hadron size ($\sim$1 fm) we obtain the equation

$$1.81\left(\frac{g^2(T_c)}{4\pi}\right)^{1/2} T_c \simeq 200 \text{ MeV}, \tag{1.20}$$

whence $T_c = 170$ MeV. The estimate is obtained using the thermodynamic potential calculated in QCD perturbation theory. At the same time it should be noted that phase transitions in QCD can be due to essentially collective phenomena which cannot be described within QCD perturbation theory.

1.4. Quasi-classical QCD methods

Among first nonperturbative effects in QCD were instantons discovered in 1975 [26]. The idea that topological vacuum fluctuations are predominant seemed at first very attractive, and many papers were devoted to this problem [27–29]. But calculations were mainly carried out in the "dilute instanton gas" approximation. As mentioned in the papers [30, 31], this approximation is however inconsistent because the instanton interaction is strong. The picture of "instanton fluid" is more realistic [32]. In this model, the QCD vacuum is rather nonuniform and instantons occupy there only a small fraction $f \sim 1/10$ of space-time. The ratio $\bar{R}/\varrho_c \simeq 3$, where ϱ_c is the characteristic instanton size, $\bar{R}$ is the mean distance between instantons. The action calculated on instanton configuration, S_0 (inst). $\gg 1$. But in stantons play an essential role, that is, there exists a strongly interacting system. This model was undoubtedly a step forward

as compared to the "instanton gas" model. What are the predictions of instanton models for QCD vacuum properties? It has apparently been reliably established recently that instantons are not directly related to the QCD confinement. The confinement is caused by some other (yet unknown) gauge field fluctuations [33]. But in QCD there exists another important problem — spontaneous chiral symmetry breaking. The success of instanton models in the solution of this problem leaves no doubt. Spontaneous breaking of chiral symmetry implies that in QCD vacuum there occurs a "quark field condensate" $\langle\bar{\psi}\psi\rangle \neq 0$. Such a condensate arises naturally in the "instanton fluid" model where the characteristic instanton size $\varrho_c \sim 1/3$ fm can be associated with the "dressed" quark size in a hadron [34]. Thus, hadron physics predicts two characteristic scales: the hadron size $r_H \sim 1$ fm and the size of a "dressed" (constituent) quark $r_Q \sim 1/3$ fm. The presence of two scales testifies in favour of the additive quark model of hadrons [35].

We have so far discussed the behaviour of instantons only at zero temperatures. If the temperature $T \to T_c$, the instanton effects vanish [36]. At $T \approx T_c$ hadrons "melt", but it is not excluded that in the course of hadron "melting" "dressed" quarks are formed, i.e. $\langle\bar{\psi}\psi\rangle \neq 0$ as before. In this case one should expect another phase transition, namely, "dressed"-bare quarks where the chiral symmetry is restored at $T = T_{\text{chir}}$. What can be the difference between the temperatures T_{chir} and T_c? In the "instanton fluid" model, $T_c \simeq T_{\text{chir}}$. A more detailed consideration to the relation between T_c and T_{chir} is given in the analysis of lattice gauge theories.

1.5. Sum rules in QCD

The sum rule method has proved very effective in the investigation of QCD vacuum characteristics [37]. This method associates the vacuum characteristics with the hadron parameters known from experiment. The essence of the method [37] is as follows. The behaviour of the correlator of two quark currents J_i, J_j: $K_{ij}(x) = \langle 0|\, T[J_i(x), J_j(0)]\, |0\rangle$ as a function of their quantum numbers i, j and the distance x is analyzed. The operation $T[\ ]$ implies time ordering of the correlator and the brackets $\langle\ \rangle$-averaging over the ensemble of gauge field configurations. The index $i(j)$ characterizes the whole set of quantum numbers, for example in the ϱ-meson channel $J^{PC} = I^{--}$, $I = 1$. Outside the light cone ($x^2 < 0$) the correlators rapidly decrease: $\sim\exp(-m|x|)$, m being the mass of the lower state in a given channel. For a Yukawa type interaction, for large x we have $\exp(-m_\pi|x|)$, where m_π is the π-meson mass. For small x in QCD there exists asymptotic freedom, and therefore the correlators can be calculated from the states of free quarks. It is well known, however, that within the applicability limits of QCD perturbation theory the nonperturbative effects play an important role. How can such effects be taken into account in calculation of the correlator K_{ij}? In the papers [37] this was done by introducing two types of phenomenological parameters — gluon and quark condensates. These parameters turned out to be quite sufficient to describe many properties of hadrons. In our opinion, it is not only the point of a suitable parametrization. The QCD interaction seems to determine the major hadron properties (for example, masses) already at small x, these properties being determined by gluon and quark field condensates. In [37], the vacuum energy density in QCD was estimated to be $\varepsilon_{\text{vac}} = -(0.5 - 1.0)$ GeV/fm^3. The vacuum energy density in the "hadron-QGP" phase transition must clearly be of the same order of magnitude.

The QCD sum rules for describing the state of the spectrum of hadron matter at finite temperatures are formulated in [38, 39]. The distinction from the case $T = 0$ consists in the fact that the correlator of currents is averaged over the ensemble of quarks and gluons in the state of local thermodynamic equilibrium at a temperature T. The analysis of the sum rules in the ϱ-meson channel [38] reveals a sharp qualitative change in the

hadron spectrum at temperatures $T_c \simeq (140-200)$ MeV testifying to the existence of the first-order phase transition responsible for deconfinement. Thus, the ϱ-meson mass turns out to be temperature-dependent (Fig. 3).

The ϱ-meson contribution to the hadron matter spectrum sharply decreases [40]. This conclusion concerning ϱ-meson "melting" at temperatures $T > T_c$ extends to other hadron resonances. This fact, important from the point of view of experimental diagnostics of QGP formation, was first explained on the basis of sum rules. Unfortunately, at finite temperatures the sum rules can be reliably employed only at a qualitative level.

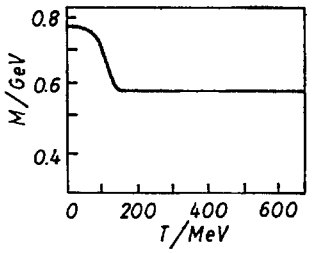

Fig. 3. Temperature dependence of ϱ-meson mass

The point is that the behaviour of quark and gluon condensates as a function of temperature is unknown. Employment of the values $\langle\bar{\psi}\psi\rangle_{T=0}$, $\langle G^2\rangle_{T=0}$ at temperatures $T \simeq T_c$ looks insufficiently correct. Nonetheless, concluding the discussion of phenomenological models of the QCD vacuum we would like to emphasize once again that in spite of the various simplifications and assumptions, all the models predict a qualitative change in the hadron spectrum at temperatures $T_c \sim 200$ MeV and energy densities $\varepsilon_c \sim$ (1-5) GeV/fm^3.

1.6. Lattice gauge theories

Successful calculations of physical quantities (including those in the strong coupling region in QCD) have been carried out in several past years within the framework of lattice gauge theories [41] (LGT). The advantages of this method are obvious because the calculations based on the QCD Lagrangian itself, nor its phenomenological replicas. The calculations are however performed by the Monte Carlo method, and one cannot always succeed in tracing the gauge field dynamics. In LGT, the continuous space-time is replaced by a lattice in Euclidean space with the number of sites N_σ in each space direction and N_β in each time direction. Each link of the lattice is assigned a certain matrix "U" from a gauge group of strong interactions. The state of the lattice is characterized by a fixed set of matrices "U" on the links, that is, a lattice is a statistical system. In the simplest case of gluodynamics (quark-free QCD), the lattice partition function has the form

$$Z(N_\sigma, N_\beta, \xi, g^2) = \int \Pi\, dU \exp\left(-S(U)\right), \tag{1.21}$$

where $\xi = a_\sigma/a_\beta$ and a_σ, a_β are distances between neighbouring lattice sites in space and time directions; $\Pi\, dU$ is the product of Haar measures corresponding to functions that realize gauge group representations; $S(U)$ is Wilson action [31] depending on the gauge field values on the links of unit squares (the so-called plackets) of the lattice in space and time directions.

The expectation value of the physical quantity X is usually determined in statistical physics using the partition function by the formula

$$\langle X\rangle = \int \Pi\, dU X(U)\, e^{-S(U)} \Big/ \int \Pi\, dU e^{-S(U)}. \tag{1.22}$$

In LGT, expressions of the type (1.22) are numerically integrated by the Monte Carlo method.

Let us now briefly discuss the results of calculations of the most interesting physical quantities. The temperature dependence of the excitation energy density for the theory based on the gauge group $SU(2)$ (free of quarks) [42–44] is plotted in Fig. 4.

First of all it is necessary to mention similarity of the results of Fig. 4 to the behaviour of the quantity ε/T^4 in the two-phase model of Sect. 1.2 (Fig. 1). At $T \sim 300-400$ MeV there occurs transition to asymptotics, i.e. to the Stefan-Boltzmann law for gluons: $\varepsilon = (4/15)\pi^2 T^4$. The expression for ε is obtained from formula (1.6) at high temperatures if in Formula (1.5) we leave only the gluon contribution and take into account that the number of gluons for the group $SU(2)$ is equal to 3. The behaviour of the energy density

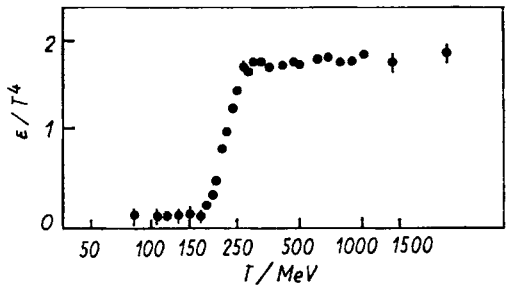

Fig. 4. Energy density as a function of temperature in $SU(2)$ gluodynamics

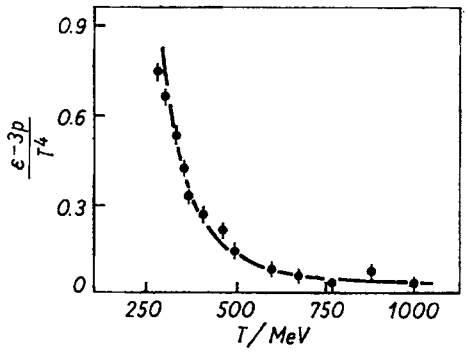

Fig. 5. Temperature dependence of interaction "strength" $(\varepsilon - 3p)/T^4$ in $SU(2)$ gluodynamics

at low temperatures corresponds to the case of "hadron" gas (see formula (1.3)). In the considered $SU(2)$ model of quark-free gluodynamics, this is a gas of colorless glueballs (in this case the quantity g_H in formula (1.3) is small). Thus, the results of Fig. 4 are surprisingly similar to the predictions of the simplest two-phase model (Sec. 1.2).

Formulas (1.4)–(1.6) of this model imply that at high temperatures there holds the equation

$$(\varepsilon - 3p)/T^4 = B/T^4. \tag{1.23}$$

The same behaviour is obtained from lattice calculations (Fig. 5). The curve in Fig. 5 corresponds to the behaviour $\sim$const$/T^4$, where const $\equiv 4|\varepsilon_{\text{vac}}|$, ε_{vac} is the vacuum energy density.

Thus, from Figs. 4, 5 one can conclude that in the theory based on the gauge group $SU(2)$, at temperatures $T_c \sim 200$ MeV there occur qualitative changes which are of the character of phase transition and lead to the formation of a non-interacting gluon gas.

The question arises whether this is a phase transition between bound colorless gluon systems (glueballs) at $T < T_c$ and quasi-free color gluons. The answer to this question could be provided by an investigation of the behaviour of the free energy F of a quark-antiquark pair put in a gluon system at a temperature T [45, 46]. The free energy F enters in the definition of the Wilson line $\langle L \rangle = \exp(-F/T)$ as order parameter. Numerical calculations reveal that $\langle L \rangle = 0$ at a temperature below T_c. This result corresponds to an infinite free energy of an isolated color quark, that is, at $T < T_c$ there exists the color quark confinement. At $T > T_c$ the line $\langle L \rangle \neq 0$, the energy $F \neq \infty$, and there occurs a phase transition into a system of quasi-free color charges. In gluodynamics based on the gauge group $SU(2)$, this is a second-order transition, i.e. there exists a peak in the specific heat of the system at $T \simeq T_c$.

We have so far considered a simplified QCD model (with a quark-free gauge group $SU(2)$). Passing over to the realistic situation — the gauge group $SU(3)$ and quark degrees of freedom, encounters a number of difficulties in LGT. The main difficulty is a correct account of virtual quark-antiquark loops in Monte Carlo method. This is now a

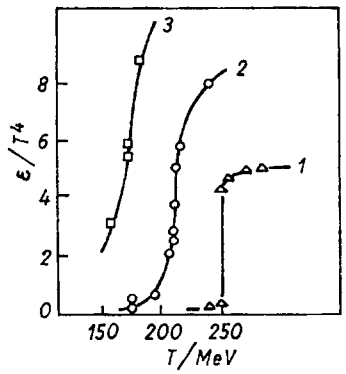

Fig. 6. Energy density of QGP as a function of temperature

"hot point" in LGT. The situation becomes more complicated because the quantitative and qualitative picture of phase transition changes through the introduction of quark-antiquark loops, as shown by calculations. Figure 6 illustrates [47, 48] the behaviour of the ratio ε/T^4 in the $SU(3)$ theory with quarks.

Curve (1) corresponds to the quark-free $SU(3)$ theory. A sharp jump is seen in the dependence $\varepsilon(T)$, which means a first-order transition. However, as quarks are involved (curves 2 and 3 differ in quark mass values), the phase transition region shifts towards lower T_c values, and the jump disappears. The first-order transition is either transformed into the second-order transition or [49] the phase transition levels up altogether and one deals with a gradual hadron transformation into a phase with free quarks and gluons. The latter process resembles, for instance, ionization of atoms. By the moment of writing this review none of the possibilities can be rejected. The development of LGT is so fast however that the dynamics of phase transition in the $SU(3)$ theory with quarks will probably be already known to the reader.

The question of the order of phase transition (or of the absence of phase transition) is not only of theoretical but also of practical interest. Indeed, in the case of first-order transition, a system of hadrons, quarks, and gluons can be in a mixed phase at a temperature T_c. Under a second-order transition, the "QGP-hadron" transition occurs as a jump at a temperature T_c. This fact may appear to be important in experimental diagnostics of QGP formation.

1.7. Chiral phase transition

Another important question connected with the account of fermion degrees of freedom in LGT is chiral symmetry in QCD. As has already been mentioned, in massless quark QCD containing no dimensional parameters two scales can be spontaneously generated: one corresponding to the confinement radius, the other to "chiral" forces binding collective QCD excitations into Goldstone bosons. Therefore, two phase transitions may occur in QCD which are characterized by two critical temperatures, T_c and T_{chir}. At a temperature T_{chir} the chiral symmetry is restored, i.e. the order parameter of fermion fields $\langle\bar{\psi}\psi\rangle_{T>T_{\text{chir}}} \to 0$. Hadrons, valence and sea quarks may also be in thermodynamic equilibrium within the temperature range $T_c < T < T_{\text{chir}}$ [40].

It should be also noted here that both instanton estimates [50] and those obtained by the sum rule method indicate that in the color charge confinement phase the chiral symmetry is broken, that is, $T_{\text{chir}} \gtrsim T_c$. But it cannot now be definitely asserted that the phase with color charge deconfinement and broken chiral symmetry ($T_c < T < T_{\text{chir}}$) also exists in QCD. Some calculations in the lattice gauge theory give the ratio $T_{\text{chir}}/T_c \simeq 1.6 \pm 0.2$ [51], other suggest $T_{\text{chir}}/T_c \simeq 1.1 \pm 0.1$ [52]. Errors in the calculations are large, and therefore it is not excluded that $T_c \simeq T_{\text{chir}}$.

2. Compression and Heating of Hadronic Matter in Nuclear Collisions

2.1. Space-time picture of hadron collisions

Before proceeding to hadron-nuclear collisions, recall a simpler space-time picture of hadron-hadron interactions. In the framework of the quark-parton model of hadrons, the interaction of hadrons in the high-energy region is assumed to proceed as follows:

1. Before collision, relativistic hadrons are ensembles of partons (valence quarks, sea quarks, antiquarks, and gluons) properly distributed with respect to the hadron momentum fraction x, carried by them. The initial distribution functions of partons can be derived from the experimental data on deep inelastic eN, μN, νN, $\bar{\nu}N$-interactions.
2. As a result of hadron-hadron interaction, part of fast protons do not participate in collective interactions and form subsequently leading secondary hadrons. Comparatively slow partons of colliding hadrons interact with one another forming a quark-gluon system whose evolution ends in the formation of the soft part of the secondary hadron spectrum.
3. Under certain conditions, multiple parton-parton collisions can lead to establishing a local thermodynamic equilibrium in quark-gluon system at an initial temperature T_i. A subsequent evolution (expansion) of the system obeys the laws of thermodynamics. The temperature in the system lowers.
4. At the final stage of evolution, at a temperature T_f, the system decays into non-interacting secondary hadrons.

In this approach to the problem there immediately arise two important questions:

1) How should one describe the transition of a quark-gluon system from the initial state (before hadron collision) to the state of thermodynamic equilibrium?
2) Whether or not the local thermodynamic equilibrium of the hadron matter is established in reality? In other words, whether the entire hadron-hadron interaction process should be described on microscopic level (in terms of the distribution function of partons) or whether there exists a time interval when macroscopic (statistical) approach can be applied to the quark-gluon system evolution.

2.2. Description of pre-equilibrium processes

2.2.1. Kinetic approach

Among the attempts to describe the kinetic processes responsible for the equilibrium state, one should mention the papers [53–55]. In these papers, the initial conditions in hadron-hadron collisions are given by the structure functions of the colliding hadrons. During the course of a hadron-hadron collision new partons are created in addition to those that already existed in the incoming hadrons. The repeated collisions between partons substantially affect their structure functions. At a final stage, quarks and antiquarks are recombined into final hadrons.

This approach is essentially kinetic and can describe experimental data on hadron-hadron interactions [53] providing one has chosen suitable "initial" structure functions. The Bratislava model can obviously be used at the equilibrium stage too if the parton kinetics is such that during the collision time it brings about statistical equilibrium of the parton system [54].

Comparison of quark densities in the central rapidity region before and after collision [56] shows that in the process of hadron collision the parton structure functions are essentially restructured. Before collision, the number of quarks per unit rapidity is about 0.6, whereas after collision the rapidity density of hadrons (mostly pions) is equal to ~ 3. Thus, in the final state the quark density makes up about 3, which is 5 times as large as that before collision.

2.2.2. Color degrees of freedom

At first glance, a rather large amount of mutual collisions of partons is required to attain thermodynamic equilibrium. For example, according to [57] this number is $\gtrsim 10$. But the number of parton collisions is not a unique important factor for the formation of local thermodynamic equilibrium. One should bear in mind that QCD partons are carriers of color degrees of freedom. Therefore already at the initial stage of hadron collision, parton distributions over x can be described by a superposition of collective and "internal" (color) motions [58]. Thus, if at the initial stage of hadron collision color degrees of freedom are excited and statistical averaging is carried our over these degrees of freedom, then the conditions for a collective (hydrodynamic) behaviour of the parton system can also be realized when the number of parton-parton collisions is small (2–3) [58].

2.2.3. The decay of a chromoelectric field

An interesting attempt to describe quantitatively the kinetic stage of hadron collision was made in [54, 55]. In the centre-of-mass system of two colliding hadrons, their interaction can be treated as a result of exchange with one or several gluons, which leads to a nonzero effective colour charge of the hadrons. In this process, a chromoelectric tube occurs which is unstable under quantum creation of quark-antiquark pairs and gluons. The produced $q\bar{q}$ pairs and gluons interact among themselves, and if the characteristic times of hadron interaction exceed the collision time of the produced $q\bar{q}$ pairs and gluons, then the system of quarks, antiquarks, and gluons can be brought into the state of local thermodynamic equilibrium. As is conventional in physical kinetics, the evolution of the quark (antiquark) distribution function is described by the Boltzmann equation [55]:

$$p^\mu \partial_\mu f(x, p) = C(x, p) + \Sigma(x, p), \tag{2.1}$$

where f is the density of quarks (antiquarks) with momentum p at the space-time coordinate x; $\Sigma(x, p)$ — the source of $q\bar{q}$-pairs, $C(x, p)$ — the collision integral. In the model [54], $\Sigma(x, p)$ characterizes the number of $q\bar{q}$ pairs produced per unit time by the homogeneous chromoelectric field. The function $C(x, p)$ is usually chosen in the approximation of relaxation time τ_i [55]. The solution of eq. (2.1) is found in [54]. The distribution function f contains two summands, the first being connected with the number of produced $q\bar{q}$ pairs, the second with the number of thermalized $q\bar{q}$ pairs. In this model there exist three characteristic time intervals: the lifetime of the chromoelectric tube under decay into $q\bar{q}$ pairs, τ_0, the characteristic collision time τ_i coinciding with the time of establishing local thermodynamic equilibrium, and the time of $q\bar{q}$ pairs system evolution under decay into final particles, τ_f. Obviously, the limit $\tau_f \gtrsim \tau_0 \gg \tau_i$ corresponds to a collisionless regime where quarks and antiquarks do not have time to achieve thermodynamic equilibrium; if however $\tau_f \gtrsim \tau_i \gg \tau_0$, then $q\bar{q}$ pairs are brought into the state of local thermodynamic equilibrium with a certain initial temperature T_i and the energy density of the quark-gluon system satisfying the Stefan-Boltzmann relation for the quark-gluon gas $\varepsilon = (\pi^2/90)\, g_Q T^4$ (see Sect. 1.2). The time values τ_f, τ_0, and τ_i are unfortunately not fixed in this model; the results depend on their relationships only. It is therefore difficult to fix uniquely the character (nonequilibrium or equilibrium) of the evolution. Clearly, the times τ_f, τ_0, τ_i are determined by the dynamics of color charge interactions in the infrared QCD region.

2.3. Thermalization time

The times of establishing local thermodynamic equilibrium are now estimated [59, 60] to be $\tau_i \simeq 1$ fm, but the accuracy of these estimates in our opinion makes up an order of magnitude, i.e. actually is must evidently be $0.1\ \text{fm} \lesssim \tau_i \lesssim 10\ \text{fm}$. If $\tau_i \simeq 10$ fm, this means that local thermodynamic equilibrium is not established in hadron-hadron collisions. The local thermodynamic equilibrium of quarks (antiquarks) and gluons cannot be perfect even in AA interactions where the interaction times make up several tens of fermi. The question of establishing local thermodynamic equilibrium in a system of interacting hadrons (and nuclei) has no unique theoretical answer at the present time. At the same time, this is a crucial point for understanding and description of hadron matter evolution. Whereas the problem of local thermodynamic equilibrium has up to now been formulated only on a theoretical level, we believe that now it has become possible to solve it experimentally. The experimental data on hh, hA, and AA interactions at high energies should be analyzed to search for the signals of local thermalization [61]. Such signals can be, provided by, $M - x$ and $P_t - x$ correlations, as well as M_t-invariance [62] in the spectra of dilepton pairs emitted by hadron matter. These signals are considered in more detail in Sec. 3.

We assume in the sequel that in hh and AA interactions, with the accelerator energies already available and also planned for the near future, local thermodynamic equilibrium is established in the hadron matter. In this case, the hadron matter evolution can be described by the statistical (hydrodynamical) methods [3, 4]. One should only bear in mind that the question of local thermodynamic equilibrium and, correspondingly, the applicability of hydrodynamics should be solved at an experimental level.

2.4. One-dimensional hydrodynamic model. Scaling-solution

Formed at an initial temperature T_i and energy density ε_i, QGP then expands and cools down. This process is natural to describe using the equations of motion of an ideal relativistic liquid [4]. In order that these equations in partial derivatives compose a closed system, they should necessarily be added with the hadron matter equation of state. It is just in setting the equation of state that the QCD predictions at finite temperatures undergo verification in comparison with experiment. If in the course of expansion the temperature T remains higher than the "QGP-hadron" transition temperature $T_c \simeq 200$ MeV, the hadron matter evolves in the quark-gluon plasma phase. When $T = T_c$, hadron formation begins, i.e. hadron matter may be in the mixed phase: QGP + hadrons. At $T < T_c$, the hadron gas undergoes hydrodynamic expansion.

Besides the equation of state, the determining role in the model predictions is played by the choice of initial (boundary) conditions that fix a unique solution of hydrodynamic equations. At the present time (see e.g. [19]) scaling initial conditions are being widely used [63, 64]. The advantage of scaling over Landau initial conditions [4] is considered in detail in [65].

The most visual picture of hadron matter evolution is provided by one-dimensional hydrodynamic expansion in scaling variables [66]:

$$\tau = (t^2 - x^2)^{1/2}, \quad \chi = \frac{1}{2} \ln \frac{t + x}{t - x}. \tag{2.2}$$

Here t and x are respectively the time and coordinate of one-dimensional expansion in the centre-of-mass system. In these variables, for the initial velocity distribution determined by a rapidity plateau:

$$Y(\chi, \tau = \tau_i) = \begin{cases} \text{const.}, & |\chi| < Y_m \\ 0, & |\chi| > Y_m \end{cases} \tag{2.3}$$

the solution of the equations of one-dimensional hydrodynamic expansion looks especially simple (scaling-solution) [64]. The temperature turns out to be only the function of the proper time of the hadron liquid element τ:

$$T(x, t) = T(\tau) \tag{2.4}$$

and not of the variable χ. The rapidities of the elements are in turn determined only by the variable χ:

$$Y(x, t) = \chi; \tag{2.5}$$

correspondingly, the velocities of matter elements are given by

$$v(x, t) = x/t = \tanh \chi. \tag{2.6}$$

The picture of hadron matter evolution in the usual variables is presented in Fig. 7. In region $0 \leqq \tau \leqq \tau_i$, hadron matter is in the nonequilibrium phase, in region $Q(\tau_i < \tau < \tau_Q)$ in the equilibrium QGP phase, M is the "mixed" phase region, H is the hadron gas. At $\tau = \tau_f$ the system decays into observed secondary hadrons. It can be readily seen that scaling solutions lead to scale-invariant spectra of secondary particles distributed

over rapidities in accordance with the Feynman plateau. This fact (along with simplicity) is just the reason for the wide usage of scaling solutions in QGP probes calculations (see Sec. 3). From the results of Fig. 7 one can imagine how difficult it is to detect QGP experimentally. Indeed, the QGP lifetime is only $\tau = \tau_Q$. Its value may turn out to be much smaller than the time τ_f (see below). The QGP formation signal will therefore be obscured by the emissions from the hadron and "mixed" phases.

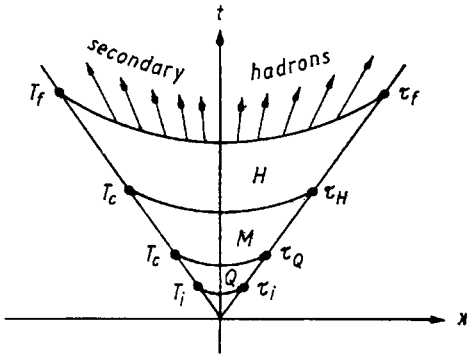

Fig. 7. Space-time evolution of QGP

2.5. Initial energy density of thermalized hadronic matter

The hydrodynamic theory of multiple production of hadrons [4] has in the past years been successfully applied to investigation of ultrarelativistic ion-ion collisions [67, 68, 59]. Let there occur a central (with a zero impact parameter) collision of two identical nuclei, with the mass numbers A, which move in the centre-of-mass system with the Lorentz factor γ ($\gamma = E/m \gg 1$, where m is the nucleon mass, E the energy per nucleon). In the longitudinal direction, nuclei undergo Lorentz contraction down to sizes $2R_A/\gamma \simeq 2A^{1/3}/m_\pi\gamma$ (R_A is the radius of the nucleus A, m_π the mass of a π-meson). At the moment $t = 0$, nucleons of colliding nuclei interact with the formation of a hadron cluster. In subsequent moments the cluster undergoes a longitudinal expansion into vacuum at a velocity of the order of that of light. Let us estimate the initial energy density of the cluster in an ultrarelativistic ion-ion interaction in the central plateau region of secondary hadron rapidities. For simplicity we replace (hypothetically) one of the nuclei by a "nucleon" moving with the Lorentz factor γ. For the $Sp\bar{p}S$ energies the height of the central plateau is $dn_{\mathrm{ch}}/dy \simeq 3$ (n_{ch} — is the number of charged secondaries). Assuming that the mean hadron energy in the plateau region $\langle E\rangle \simeq 400$ MeV, and the neutral-to-charged particle ratio $n_0/n_{\mathrm{ch}} \simeq 0.5$, we find the energy density within the rapidity interval from y to $y + dy$:

$$\frac{d\langle E\rangle}{dy} \simeq \frac{3}{2}\frac{dn_{\mathrm{ch}}}{dy}\langle E\rangle \simeq 1.8\ \mathrm{GeV}. \tag{2.7}$$

If the incident particle is not a nucleon but a nucleus, then in the approximation of non-interacting A nucleons the energies of the hadrons produced in the rapidity interval from y to $y + dy$ should be added. Let us evaluate the energy density at the moment of establishing thermodynamic equilibrium for a hadron cluster of $2\Delta x$ in thickness between two boundaries (flat layers) moving at velocities $v = \pm\Delta x/\Delta t$. According to the scaling- olution, the secondary hadrons that correspond to this layer will be bound within the rapidity interval $\Delta y = 2\,\mathrm{arctanh}\,(\Delta x/\Delta t) \simeq 2\Delta x/\Delta t$. In the approximation of non-

interacting secondary hadrons, the energy in the layer will be

$$E = A \frac{d\langle E\rangle}{dy} \Delta y. \tag{2.8}$$

To determine the initial energy density ε_i, one should divide the energy (2.8) by the initial volume: $\varepsilon_i = E/V_i$. To calculate the cluster volume at the thermalization moment τ_i, we will use the scaling variables (2.2). In these variables, the element of 4-volume makes up

$$d^4x = d^2x_t \, d\chi\tau \, d\tau. \tag{2.9}$$

Integrating (2.9) over χ in the limits $\pm\Delta y/2$, we find

$$V_i = \pi R_A^2 \tau_i \, \Delta y_i \tag{2.10}$$

where πR_A^2 is the cross-section of the colliding nuclei,

$$R_A = 1.2\,\text{fm} \cdot A^{1/3}, \pi R_A^2 = 4.5\,\text{fm}^2 \cdot A^{2/3}. \tag{2.11}$$

Then the initial energy density is [59]:

$$\varepsilon_i \simeq \frac{A^{1/3}}{4.5\,\text{fm}} \cdot \frac{d\langle E\rangle}{dy} \cdot \frac{1}{\tau_i}. \tag{2.12}$$

For a uranium nucleus, e.g., the initial energy density of a nuclear matter for characteristic times of thermalization $\tau_i \sim 1$ fm, is estimated to be

$$\varepsilon_i \simeq 5\ \text{GeV/fm}^3. \tag{2.13}$$

This energy density is by about an order of magnitude higher than the nucleon energy density in nuclei, and as has been mentioned in Sec. I, for such energy densities one should expect transition of nuclear matter into quark-gluon plasma.

An important consequence of formula (2.12) is an increase of the initial energy density as $A^{1/3}$ with increasing atomic number of the colliding nuclei. The reason for this dependence is that the initial conditions for hydrodynamic expansion at the time $\tau_i \simeq 1$ fm in a central collision of nuclei arise from $A^{1/3}$ pairs of nucleon-nucleon collisions (inside the "nuclear tube"). Important are the questions, in what volume the energy density (2.13) can be generated and whether the available accelerator energies are sufficient to generate the required energy density. At first sight the energies do suffice. The CERN collider give the energy ~ 540 GeV to particles in the centre-of-mass system. If all this energy were converted to heat and the energy density reached the values (2.13), then, as can be easily estimated, the excited cluster would have the volume $V_i \simeq 500\,\text{fm}^3$, i.e. would be comparable with the volume of heavy nuclei. The initial hadron energy is however not completely converted into "heat" in real collisions. The point is that about half the energy is carried away by "leading nucleons", the rest being expended mostly to pion production, but the energy distribution is nonuniform. At collider energies, the number of charged particles produced in unit rapidity is $dn_{\text{ch}}/dy \simeq 3$, as has been mentioned above. If one is interested in the events in experiments in which hadron matter is transformed into quark-gluon plasma, i.e. a substantial entropy is generated, one should take care in the choice of events. So, to identify events with large ε_i, one should take "central" collisions of nuclei. Among the events thus chosen, one should in turn identify those with a high entropy generation, for example, with high values of dn_{ch}/dy. It cannot be said definitely which particles (constituent quarks, current quarks, gluons) can

generate the energy density (2.13). In any case it should be expected that particles in a hadron cluster undergo repeated collisions which result in local thermodynamic equilirium with the initial temperature T_i.

2.6. Initial entropy density

We will try to associate the initial temperature T_i with the characteristics of secondary hadrons and estimate the times τ_Q, τ_H, and τ_f in the case of entropy conservation. The latter assumption suggests an ideal QGP expansion (the dissipative summands in the QGP energy-momentum tensor are disregarded).

Suppose, two identical nuclei of radius R_A collide with the formation of thermalized QGP, as in Sec. 2.5. In the longitudinal direction QGP is distributed as shown in Fig. 7, and in the transverse direction it occupies at cylinder of radius R_A. We assume for simplicity that QGP expands only in the longitudinal direction in accord with the scaling-solution of Sec. 2.4. Using the equation of state of an ideal QGP gas in the model (1.1)–(1.3), we find the QGP entropy density

$$s = (\varepsilon + p)/T = dp/dT = 4\pi^2 g_Q T^3. \tag{2.14}$$

According to the scaling-solution (2.4), the entropy density depends only on the proper time: $s(x, t) = s(\tau)$, then at the time τ the total entropy is $S = s(\tau)\, V(\tau)$, where $V(\tau) = \int d^4x' \delta(\tau - \tau')$. Integrating over d^4x' according to (2.9) and (2.3), we find $V(\tau) = \pi R_A^2 \tau 2Y_m$. Whence

$$S = \pi R_A^2 2Y_m\, S(\tau)\, \tau = \pi R_A^2 4\pi^2 g_Q T^3 \tau 2Y_m. \tag{2.15}$$

To relate the entropy S with the observed quantities, we assume the QGP expansion to proceed adiabatically in the "mixed" and hadron phases, i.e. the entropy S is constant. Since in the hadron phase the pion gas expansion obeys the state equation (1.1)–(1.3), then by analogy with (2.15) we have in this phase

$$S = 4\pi^2 g_H \pi R_A^2 2Y_m T^3 \tau, \tag{2.16}$$

where $\tau > \tau_H$. In particular, at the moment of system decay into observed hadron ($\tau = \tau_f$):

$$S/2Y_m \cong dS/dy \cong c\, dn_\pi/dy \tag{2.17}$$

where $c \cong 3.6$; dn_π/dy is distribution over the rapidities of π-mesons produced in AA interaction.

Comparing (2.15) and (2.17), we obtain the relation of the initial entropy density with the observed quantities [69]:

$$s_i = \frac{c}{\tau_i} \frac{1}{\pi R_A^2} \frac{dn_\pi}{dy} = \frac{1.2\ \mathrm{fm}^{-2}}{\tau_i A^{2/3}} \frac{dn_{\mathrm{ch}}}{dy}. \tag{2.18}$$

It should be emphasized that entropy density is meaningful only in the presence of local thermodynamic equilibrium. Contrary to entropy, the energy density (2.12) can be determined in a nonthermalized medium. Using (2.18), we find the relation of the initial

temperature with τ_i [69]:

$$T_i = \left[\frac{1.2\,\text{fm}^{-2}}{4\pi^2 g_Q \tau_i A^{2/3}} \frac{dn_{\text{ch}}}{dy}\right]^{1/3} \tag{2.19}$$

As is seen from this relation, the initial temperature T_i depends on the QGP thermalization time τ_i. It has already been mentioned above that the time τ_i is uncertain.

The time τ_i may depend, in particular, on the atomic number of the nucleus. For example, the parametrization $\tau_i^{AA} = \tau_i^{pp}/A^{\delta}$, $0 < \delta < 1/3$, and $\tau_i^{pp} = 0.5$ fm is used in [70]. With such estimates it is difficult to expect accuracy higher than an order of magnitude. From the expression (2.19) it follows that T_i is determined up to the factor ~ 2. As an example [69] consider collision of O^{16} with a Pb nucleus with $dn_\pi/dy = 42$. Using (2.11)–(2.19), we obtain the thermalization time $\tau_i \simeq 0.1$ fm, $T_i \simeq 320$ MeV, the initial energy density $\varepsilon_i \simeq 17$ GeV/fm^3. The lifetime of the quark phase $\tau_Q = 0.8$ fm, $T_c = 160$ MeV, $\varepsilon_Q = 1.4$ GeV/fm^3. In the mixed phase the energy density $\varepsilon \simeq 0.1$ GeV/fm^3. The hadron phase has $\tau_f \simeq 14$ fm, $T_f \simeq m_\pi \simeq 140$ MeV, $\varepsilon_f \simeq 12\ m_\pi^4$.

In spite of uncertainty of the estimates, this example shows how short the QGP lifetime may appear to be and how difficult it is to identify a QGP signal against the background of the hadron and possibly also "mixed" phases.

2.7. Dissipative processes

In estimating the quantities ε_i and T_i we have used the ideal fluid approximation. Note that this approximation for quarks and gluons does not imply that the interacting in the system is small. It is of importance that the interaction be properly taken into account by the equation of state $p = p(\varepsilon)$. Among the papers devoted to this topic we should mention [71–73]. As is well known, the ideal fluid approximation is applicable if the characteristic times and free paths of particles (in the case of quarks, antiquarks, and gluons) in the system satisfy the conditions

$$\begin{cases} \tau \ll t \\ \lambda \ll L \end{cases} \tag{2.20}$$

where t and L are the time and scale factors on which such macroscopical hydrodynamic quantities as energy density, pressure, etc. change considerably. To what degree is this picture valid for ultrarelativistic ion-ion interactions? Since the characteristic free paths of quarks $\lambda \lesssim 1$ fm and the system dimension in the transverse direction $R_A \sim A^{1/2}$ fm, the conditions (2.20) are fulfilled within a reasonable accuracy. The condition that the hadron liquid be ideal is, of course, not obligatory. Nuclear (hadron) matter may exhibit viscosity. This fact can be taken into account by adding to the right-hand side of the equation of motion for the energy-momentum tensor $\partial_\mu T^{\mu\nu} = 0$ a term that takes into account the energy dissipation under hydrodynamic expansion [54]. An account of nuclear matter viscosity decreases the initial energy density in AA interactions down to values $\varepsilon_i \simeq (1-2)$ GeV/fm^3 [54], but even with such ε_i values the nuclear matter is able to be in the quark-gluon plasma phase.

Concluding this section, we would like to emphasize once again that in spite of the approximate character of the estimates of initial energy densities and temperatures of a nuclear cluster, the indicated hadron → quark-gluon plasma transition can be achieved in ion-ion collisions ($A \gtrsim 10$) for energies $E_{\text{c.m.}} \gtrsim 10$ GeV/nucleon in the centre-of-mass system.

3. Experimental Signals of QGP Formation

3.1. QGP diagnostics

In the preceding sections are given theoretical considerations testifying in favour of QGP formation in ion-ion collisions for energies $E_{c.m.} \gtrsim 10$ GeV/nucleon. In this section we discuss the dynamical processes in QGP under its hydrodynamic expansion and the experimental manifestations of these processes. The goal of QGP diagnostics resembles in a sense the problems of the Universe origin: the initial conditions should be reconstructed from data of observational astronomy (far-reaching effect of Big Bang).

Of particular importance is to find out which observed characteristics of collisions carry information on QGP formation.

Among the experimental QGP signals reported in the literature, we will single out the following:

a) The analysis of the spectra of leptons, photons, and J/ψ-particles produced at the QGP stage and undergoing no subsequent interactions can be used to trace the properties of matter at hottest stage, e.g., QGP temperature.
b) Hadron transverse momentum dependence on dn/dy probes the QGP — hadron phase transition.

In the discussion of these problems, the most detailed consideration is given to the formation of lepton pairs in QGP. On this example we demonstrate the typical problems and difficulties encountered in QGP diagnostics. These problems are inherent in all QGP signals and connected with the following two facts.

Quark-gluon plasma is a macroscopical ensemble characterized by temperature, pressure, chemical composition (the number of different types of particles), etc. In the process of nuclear collisions it exists, however, in a finite temperature interval $T_i > T > T_c$ (see Fig. 7); when under hydrodynamic expansion the temperature falls below T_c, QGP is transformed into hadrons. Soft processes of hadronization may substantially distort information on parton system evolution. This is just one of the QGP diagnostics problems: since the parton hadronization mechanism is still unknown, the results of decoding of observed inclusive hadron spectra, as well as other hadron characteristics, in search for QGP signals are model-dependent and cannot serve as a rigorous proof of QGP existence.

Another unfavourable circumstance is that the dimensions of the space-time region occupied by QGP in the course of system evolution are smaller than the 4-volume of the hadron (and mixed) phases. Experimental QGP signals can therefore be obscured by the hadron phase.

One should bear in mind that a possible QGP signal distortion during subsequent evolution as well as the signal-background relation have not yet been studied in detail. Preliminary results of such investigations show that initially optimistic tones with respect to several reported signals of QGP formation is often followed by dissappointment.

3.2. Lepton pair production

3.2.1. QGP signal calculations

Detection of electromagnetic signal by a hot hadron matter was proposed as far back as 1959 [74]. Such a QGP signal may be lepton pairs $\mu^+\mu^-$, e^+e^-, photons γ. The advantage of these particles from the viewpoint of QGP diagnostics is that they leave the QGP

volume undergoing practically no secondary interactions with quarks and gluons (contrary to hadrons).

The general algorithm of calculating the QGP signal characteristics is as follows. It is necessary first to obtain the probability of particle formation per unit time in unit volume in the rest frame of the element of a quark-gluon matter and then to integrate over the 4-volume with an account of the "history" of system evolution. Note that the particle production rate in the rest frame of the element of the QGP is determined by quantum electrodynamic or quantum chromodynamic formulae and is rather exactly known at least at high temperatures. At the same time, integration over the system evolution is model-dependent due to unsertainties in the initial conditions (scaling or other), type of expansion (one- or three-dimensional), etc. In view of these uncertainties, the relation of QGP and hadron phase signals cannot be reliably estimated.

3.2.2. Annihilation cross-section

Consider in more detail the dilepton production by a thermalized medium. Such a medium can be either quarks, antiquarks, and gluons in the deconfinement phase or the hadron (pion) gas. In first-order perturbation theory, the dilepton production is described by the diagram of Fig. 8, where "q" is a pion or a quark.

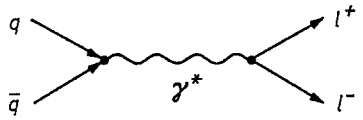

Fig. 8. Production of lepton pair

In quantum electrodynamics, the annihilation e^+e^- is similar to that shown in Fig. 8. The cross-section of the annihilation $e^+e^- \to \mu^+\mu^-$ is of the form

$$\sigma(M) = \frac{4\pi}{3}\frac{\alpha^2}{M^2}\left(1+\frac{2m^2}{M^2}\right)\left(1-\frac{4m^2}{M^2}\right)^{1/2}, \tag{3.1}$$

where α is the fine structure constant, m the muon mass, M the mass of a virtual photon γ^*. In the case of quark and antiquark annihilation, one should take into account the color factor $N_c = 3$ in formula (3.1). Besides, one should bear in mind that quarks have a fractional electric carge ($e_u = 2/3$, $e_d = -1/3$). Then the e^+e^- — pair production cross-section by quark and antiquark is given by

$$\sigma_q(M) = F_q\sigma(M), \tag{3.2}$$

where $F_q = 4N_c \sum_f e_f^2$, the summation being carried out over the quark flavours. In this expression we have also summed up over the spins of quarks in the initial state. Formulas (3.1) and (3.2) require some complication if particles a and $\bar{a}$ (Fig. 8) are pions. Since pions are colourless spinless particles with unit electric charge, the factor of averaging over spin and colour gives unity. By the vector dominance hypothesis, the main $\pi^+\pi^-$-annihilation channels are $\pi^+\pi^- \to \varrho \to e^+e^-$, $\pi^+\pi^- \to \varrho' \to e^+e^-$. It is therefore necessary to multiply (3.1) by the form factor which is the sum of Breit-Wigner resonances:

$$F_\pi(M) = \frac{m_\varrho^4}{(m_\varrho^2 - M^2)^2 + m_\varrho^2\Gamma_\varrho} + 0.25\,\frac{m_{\varrho'}^4}{(m_{\varrho'}^2 - M^2)^2 + m_{\varrho'}^2\Gamma_{\varrho'}^2}, \tag{3.3}$$

$m_\varrho = 775$ MeV, $\Gamma_\varrho = 155$ MeV; $m_{\varrho'} = 1600$ MeV, $\Gamma_{\varrho'} = 260$ MeV.

The factor 0.25 arises due to the fact that the branching of they decay $\varrho' \to \pi^+\pi^-$ makes up 25%. Thus, the cross-section of the process $\pi^+\pi^- \to e^+e^-$ is determined by the expression

$$\sigma_\pi(M) = F_\pi(M)\,\sigma(M)\left(1 - \frac{4m_\pi{}^2}{M^2}\right)^{1/2}. \tag{3.4}$$

3.2.3. The annihilation rate in a matter

To calculate the probability of dilepton production per unit time in unit volume of a thermalized matter, the annihilation cross-section $\sigma(a\bar{a} \to e^+e^-)$ should necessarily be averaged over the momentum distribution functions of primary particles (f) and antiparticles ($\bar{f}$):

$$R(a\bar{a} \to e^+e^-) = \int \frac{d^3p}{(2\pi)^3} f(p) \int \frac{d^3\bar{p}}{(2\pi)^3} \bar{f}(\bar{p})\,\sigma(a\bar{a} \to e^+e^-)\,v, \tag{3.5}$$

where v is the relative velocity of the primary particle and antiparticle, $v = [(E\bar{E} - p\bar{p})^2 - m_a{}^4]^{1/2}/E\bar{E}$, E and p ($\bar{E}$ and $\bar{p}$) being the energy and momentum of particles (antiparticles). In what follows we will be concerned with the case $T \gtrsim m_a$, then we may approximately assume that

$$f(p) \simeq \exp(-E/T). \tag{3.6}$$

In this case, integration of the expression (3.5) gives the equality

$$\frac{dN}{d^4x\,dM^2\pi\,dP_t{}^2\,dY^*} = \frac{\sigma_a}{(2\pi)^5}\left(1 - \frac{4m_a{}^2}{M^2}\right)\exp(-E^*/T), \tag{3.7}$$

for the number of lepton pairs, with invariant mass M, emitted from the element d^4x of the 4-volume. In (3.7), P_t is the transverse momentum of the dilepton, Y^* and E^* are respectively the rapidity and energy of the dilepton in the rest frame of the QGP element: $E^* = E + \bar{E} = M_t \cosh Y^*$, $M_t = (M^2 + P_t{}^2)^{1/2}$ is the "transverse" mass of the dilepton.

3.2.4. System evolution

The expressions (3.7) and (3.8) solve the first part of the problem, i.e. assist in calculating dilepton pair generation in the rest frame of the element of the matter. However, as has been mentioned above, QGP undergoes hydrodynamic expansion in the course of evolution (Fig. 7). Under one-dimensional hydrodynamic expansion, integration of the expression (3.7) over d^4x (2.9) leads to the formula for dilepton production cross-section in QGP ($m_q = 0$):

$$\frac{d\sigma}{dM^2\,d^2P_t\,dy} = \frac{\sigma_q}{(2\pi)^5}\pi R_A{}^2 \int_{\tau_i}^{\tau_0} \tau\,d\tau \int_{-Y_m}^{Y_m} d\chi \exp\left(-\frac{M_t \cosh(y-\chi)}{T}\right). \tag{3.8}$$

In this formula, as distinguished from (3.7), y is the dilepton rapidity in the centre-of-mass system of AA collision, $y = Y^* + \chi$. In setting the integration limits, the scaling conditions (2.3) as well as the lifetimes of QGP phase are taken into account (Fig. 7). For $y \ll Y_m$ ($y \simeq 0$), integration over χ gives

$$\int d\chi \exp\left(-\frac{M_t \cosh\chi}{T}\right) \simeq 2K_0\left(\frac{M_t}{T}\right) \simeq \left(\frac{2\pi T}{M_t}\right)^{1/2} \exp\left(-\frac{M_t}{T}\right). \tag{3.9}$$

According to the scaling-solution (2.6), the proper time is in one-to-one correspondence with the temperature $\tau T^3 = \tau_i T_i^3$ (see Sec. 2.6), whence $\tau\, d\tau = T_i^6 \tau_i^2\, 3dT/T^7$. Thus, from (3.8), we derive [62, 69]

$$\frac{d\sigma}{dM^2\, d^2P_t\, dy} = \frac{\sigma_q}{(2\pi)^5}\, \pi R_A^2 3 T_i^6 \tau_i^2 \int_{T_c}^{T_i} \frac{dT}{T^7} \left(\frac{2\pi T}{M_t}\right)^{1/2} \exp\left(-\frac{M_t}{T}\right). \tag{3.10}$$

Formulas for the contributions into the dilepton production cross-section from the pion and mixed phases can be obtained in a similar manner [75, 76].

3.2.5. Properties of QGP produced dileptons

The formulas derived in the preceding section make it possible to calculate the behaviour of the spectra of dileptons generated in QGP. Before normalization, we consider several semi-qualitative characteristics of the behaviour of these spectra, which can serve for QGP diagnostics.

Figure 9 (from ref. [77]) shows the behaviour of the dilepton mass spectra as predicted by the QGP model. Note that for masses 1 GeV $< M <$ 3 GeV such a behaviour coincides with the experimental data on dilepton production in pA interactions. As is

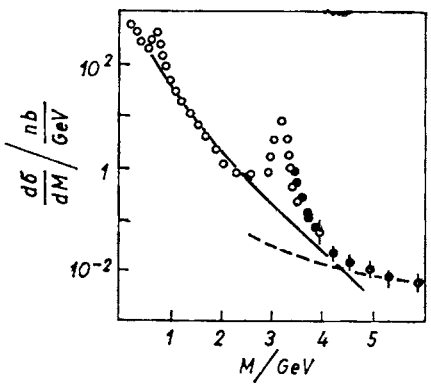

Fig. 9. Dimuon mass spectrum in proton-nucleon interactions at 225 GeV (open circles) and 400 GeV (closed circles). Solid line corresponds to QGP rate [77], dashed line to Drell-Yan process

known, for dilepton masses $M > 3$ GeV the behaviour of the spectrum is described well by the Drell-Yan mechanism (annihilation of quarks and antiquarks of colliding hadrons). The contribution of this process is shown in Fig. 9 by the dashed line. As follows from Fig. 9, for masses $M \lesssim 3$ GeV this mechanism does not already describe dilepton production. An especially large difference (about 100 times) is observed for masses $M \lesssim 0.6$ GeV. Dileptons in this mass region are called "anomalous". The origin of "anomalous" dilepton pairs is not yet known. A possible relation of "anomalous" dileptons with the electromagnetic QGP signal was discussed in [78–80]. Experimental data on "anomalous" dileptons can be found in Fig. 10 (ref. [78]).

The spectra of dileptons produced in QGP at $T_i = 180$ MeV and $T_c = 160$ MeV are given for comparison. From this figure it follows that the mass spectra of "anomalous" dileptons agree qualitatively with QGP predictions.

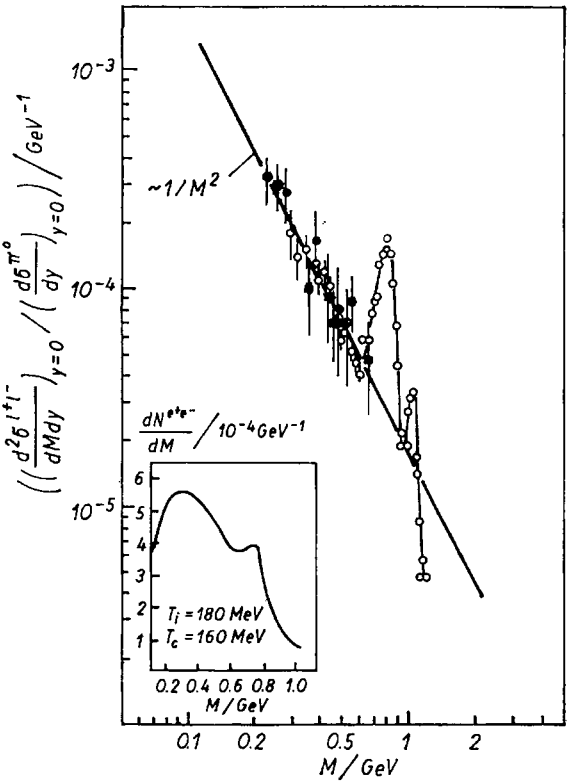

Fig. 10. Lepton pair cross-section (normalized to pion density at $y = 0$) as a function of pair mass

Formula (3.10) implies that the spectra of dileptons due to QGP possess the M_t-scaling property, i.e. the spectra depend not separately on the variables M_t and P_t, but on their combination M_t. The distribution of dileptons from QGP over the variable M for fixed values of M_t, y must therefore be close to a constant. Indeed, Fig. 11 from ref. [62] shows that in the nonresonant region 1.2 GeV $< M <$ 2.7 GeV the dimuon production cross-section at fixed M_t is independent on M. For the same M_t variation the absolute value of the differential cross-section changes by several orders of magnitude! Similarly, the dilepton distribution over P_t for fixed M_t and y values must also be constant. On the contrary, the same distribution of dileptons produced at a pre-equilibrium stage in the model [54] (Sec. 2.2.3) is different from constant [81] (Fig. 12). This fact may help in identification of dilepton production mechanisms in hadron collisions.

But the M_t-scaling is inherent not only in thermodynamic models. For example, inclusive spectra of particles produced through the Regge mechanism of Kancheli-Mueller [82] in the central region possess the same properties.

Some authors [62, 69] propose to use a more detailed prediction — a power-law decrease of the spectra in the mass region 1 GeV $< M <$ 2 GeV as a possible experimental signal of QGP generation in ion collisions. Formula (3.10) implies that this decrease can be given by

$$\frac{d\sigma}{dM^2\, dP_t^2\, dy} \sim \frac{1}{M_t^6}. \tag{3.11}$$

But in the mass interval 1 GeV $< M <$ 2 GeV, the spectra of dileptons from a pre-equilibrium stage, which are calculated in the model [54], also decrease by the law $\sim 1/M_t^6$ [81]. Since at the present time there are no criteria for choosing one of the two mechanisms, the functional dependence (3.11) is of no help in choosing either QGP or nonequilibrium phase as the sourse of lepton pairs.

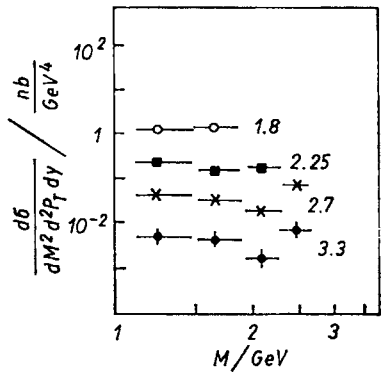

Fig. 11. Dimuon spectrum is independent of mass if the transverse mass is fixed [62]. The values of M_t/GeV is shown near corresponding data points (read t instead of T)

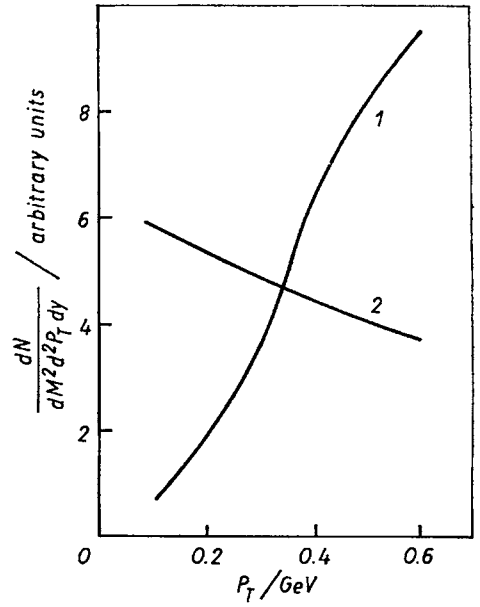

Fig. 12. P_t-spectrum of dileptons produced by chromoelectric flux tubes at fixed value of $M_t = 0.65$ GeV and $|y| < 0.5$. Curves 1 and 2 correspond to different types of source in eq. (2.1) (read t instead of T)

3.2.6. Correlation in dilepton spectra

In the derivation of the relations (3.9) and (3.10), local thermodynamic equilibrium with an initial temperature T_i was assumed to be established in a system of quarks, antiquarks, and gluons for a time τ_i. It should be stressed that the fact of establishing any temperature in QCD is far from being obvious by itself. Indeed, the possibility of finding the temperature in the thermodynamical sense (or impossibility of introducing this characteristic) it not efficiently ascertained by QCD dynamics known well in the strong coupling region. At this stage, we think it reasonable to solve the problem of thermalization experimentally. Since dileptons and photons are effectively emitted also at times close to τ_i (contrary to hadrons), their spectra must be sensitive to the assumption of thermalization.

In an equilibrium QGP, the dilepton production cross-section is mainly specified by the Boltzmann factor (see formula (3.7))

$$\exp(-E^*/T_c) \simeq \exp\left(-(M^2 + P_t^2 + P_l^{*2})^{1/2}/T_c\right), \tag{3.12}$$

which arises from the product $f(E)\,\bar{f}(\bar{E})$ of the distribution functions of quarks and antiquarks. In formula (3.12), $P_l^* = M_t \sinh Y^*$ — is the longitudinal momentum of a dilep-

ton in the rest frame of the QGP element. The Boltzmann factor leads to the following correlation in the spectrum of dileptons produced in an equilibrium QGP: the dilepton pair distributions over P_t (over M) become harder with increasing longitudinal dilepton momentum P_l^* observed in c.m.s., i.e. the relative part of high values of transverse momenta (masses) increases. Indeed, an analysis of formula (3.12) readily shows that dilepton distributions over P_t and M are distinct for distinct P_l^* values. In selection of events with high P_l^* values in these distributions, the fraction of high mass and P_t

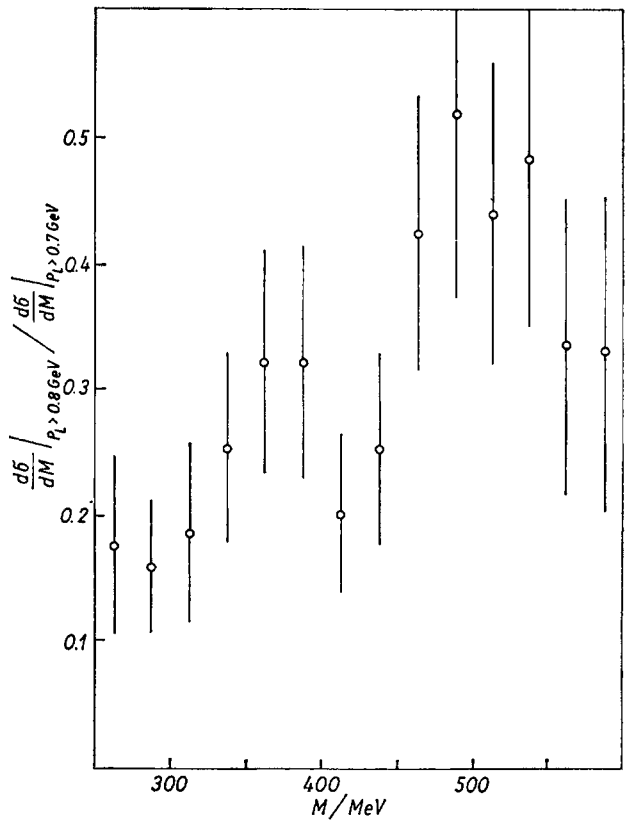

Fig. 13. Ratio of dumuon mass spectra measured at different c.m.s. longitudinal momenta P_l^*

values increases. The observed longitudinal momentum of the dilepton produced in the QGP model is determined both by the local value of the momentum P_l^* and by the hydrodynamic QGP expansion $P_l = M_t \sinh(Y^* + \chi)$. For large transverse dilepton masses M_t, the characteristic "thermal" rapidity values Y^* will be much lower than the values acquired under hydrodynamic expansion. The observed longitudinal momentum P_l will not therefore be related to P_l^* value, and thus the "thermal" $P_t - P_l(M - P_l)$ correlations will be absent. For small M_t, the situation is vice versa. In this case, selection of events with large P_l effectively selects dileptons with large P_l^*, and the indicated correlations occur.

Such $P_t - P_l$ correlations are absent in the spectra of dileptons produced in a non-equilibrium phase [81]. Thus, an experimental discovery of $M - P_l$ and $P_t - P_l$ corre-

lations in dilepton spectra in the mass interval 0.1 GeV $< M <$ 0.6 GeV would permit identification of the dilepton production mechanism (equilibrium and nonequilibrium), i.e. would serve as a signal of thermalization in processes under study.

An example of experimentally observed $M - P_l$ correlations may be the difference in the mass distributions of "anomalous" dimuons measured for different values of $x = 2P_l/\sqrt{s}$ in [83] and [84] (see also [85]). This difference is shown in Fig. 13: the part of events with large masses increases with increasing longitudinal momentum P_l. Such an effect may be an indication of the existence of local thermodynamic equilibrium in hadron collisions.

3.2.7. The density ratio dn/dy for dileptons and pions

A great progress in removal of uncertainties in dilepton spectra normalization in QGP is achieved provided that entropy is conserved in the course of system evolution (Sec. 2.5.3). The idea is to construct a τ_i-independent quantity from experimentally observed spectra [76, 86]. To this end, we find from (3.10) the number of dileptons dn_{ll}/dy produced per unit rapidity. The quantity dn_{ll}/dy is proportional to τ_i^2 (consequence of formula (2.19)), and the multiplicity of charged pions $dn_{\mathrm{ch}}/dy \sim \tau_i$, and therefore the ratio $\dfrac{dn_{ll}/dy}{(dn_{\mathrm{ch}}/dy)^2}$ does not depend on τ_i. This ratio is presented in Fig. 14 [76].

The ratio turns out to be a monotonously increasing function of dn_{ch}/dy if there exists only a pion phase in thermalized state. If the initial energy density exceeds the QGP for-

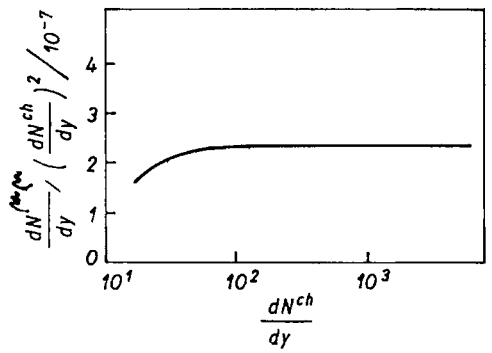

Fig. 14. Ratio of a dilepton rapidity density to a hadron rapidity density squared is constant in QGP model (read $n_{\mu\mu}$ instead of $N^{\mu\mu}$, n_{ch} instead of N^{ch})

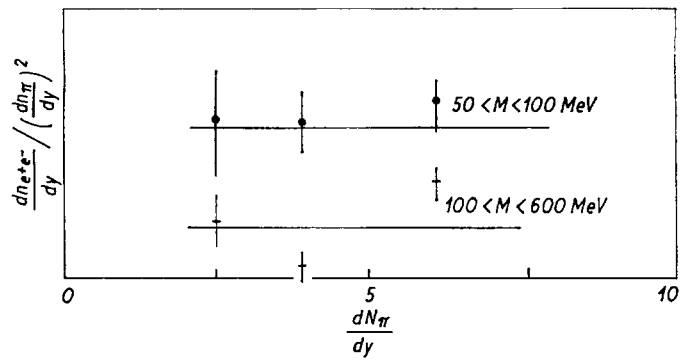

Fig. 15. Yield of dileptons divided to a square of pion density is independent of dn_π/dy [87] (read n_π instead of N_π)

mation threshold ($\varepsilon_i \simeq 1 - 2$ GeV), this ratio goes onto a plateau, the plateau height being proportional to the phase transition temperature T_c. An experimental measurement of the ratio $\frac{dn_{ll}/dy}{(dn_\pi/dy)^2}$ as a function of dn_π/dy seems to be of great importance from the viewpoint of the diagnostics of QGP formation in ion collisions.

Figure 15 presents the ratio $(dn_{e^+e^-}/dy)/(dn_\pi/dy)^2$ as a function of dn_π/dy at $y = 0$ from the data of AFS collaboration [87]. The independence of this ratio implies that "anomalous" dileptons are produced at an intermediate stage of hadron interaction. In other words, the mechanism of their production is related neither to the Drell-Yan process at the initial interaction stage nor to the decays of or bremsstrahlung radiation by final-stage hadrons [88].

3.2.8. Uncertainties in QGP signal normalization

In spite of the substantial decrease of uncertainty in the normalization of formula (3.10) attained by using the relation (2.13), the inexact values of τ_i and the initial QGP volume lead to a considerable uncertainty in the estimate of the quark and hadron phase contribution into the dilepton spectrum. Obviously, the quark phase contribution into the dilepton spectrum is enhanced for $\tau_i \simeq 0.1$ fm, while the hadron phase contribution for

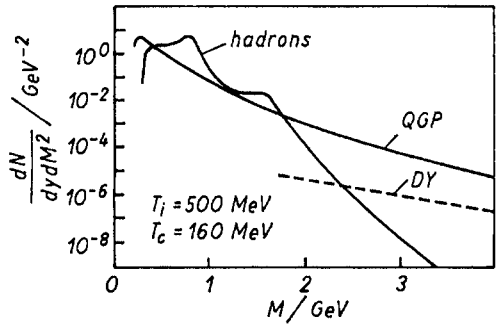

Fig. 16. Contribution to dilepton mass spectrum from QGP and hadron phases (dashed line-Drell-Yan process contribution) (read $n_{\mu\mu}$ instead of N)

$\tau_i \simeq 10$ fm. As an illustration, Fig. 16 presents the $\mu^+\mu^-$ spectra [76] in central collisions of ^{197}Au nuclei for energies $E \gtrsim 50$ GeV/nucleon in the centre-of-mass system. The parameter τ_i is chosen to be equal to 1; $\pi R_A^2 = 127$ fm^2.

From these figures it is seen that the pion phase dominates over the quark phase in the region $M \lesssim 2$ GeV. The quark component becomes noticeable for $M \gtrsim 2$ GeV because, as is seen from Fig. 7, quarks and antiquarks annihilate on the average at higher temperatures than pions. It should be stressed once again that these assertions refer to the value $\tau_i \simeq 1$ fm. If τ_i approaches ~ 0.5 fm, then the quark component starts dominating over the hadron one in the dilepton spectra also for $M \lesssim 2$ GeV. Thus, the exact form of dilepton spectrum cannot be a priori predicted in real experiments. Everything is ultimately determined by the relationship between the lifetimes of the two phases.

3.2.9. "Melting" of resonances

Comparing the expressions (3.9) and (3.10), one can notice an important feature of dilepton spectra. In the spectra of dileptons produced in the pion phase, strong peaks corresponding to ϱ, ϱ', and to other resonances are observed, whereas the spectra of dileptons

produced in QGP exhibit no such peaks. The higher the temperature $T_i > T_c$, the less pronounced the resonance peaks in the dilepton spectrum. The resonances seem to "melt" in QGP [40]. An example [76] of this "melting" is presented in Fig. 17.

Since the transverse hydrodynamic expansion was disregarded, the "transverse" mass M_t of a dilepton pair increases with temperature at which this pair was produced. Quark-antiquark annihilation dominates at $T > T_c$ and pion annihilation at $T < T_c$. Therefore, the relative contribution from the pion phase decreases with increasing M_t. In a number of papers [38, 40], resonance "melting" is associated with restoration of

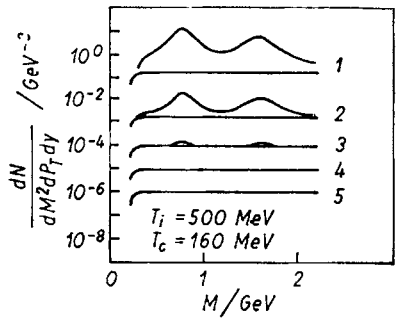

Fig. 17. "Melting" of resonances in dimuon spectrum as M_t increases. The values of M_t/GeV are shown near the curves (read $n_{\mu\mu}$ instead of N, t instead of T)

chiral symmetry in quark-gluon plasma, i.e. with disappearance of the condensate of quark fields $\langle\bar{\psi}\psi\rangle$. This effect could be rather instructive from the viewpoint of QGP formation diagnostic, but it depends on the QGP expansion model. Indeed, [89], in the (3 + 1)-dimensional expansion model, the transverse expansion rate increases with time, whereas the temperature falls. And since in the pion phase dileptons are mainly produced at the final stage of expansion, the resonance "melting" in a real (3 + 1)-dimensional expansion model must be less pronounced than in the (1 + 1)-dimensional scaling model.

3.3. Emission of J/ψ particle

Alongside dileptons, which undergo practically no rescattering in QGP and are therefore able to be its "thermometer", this property is also inherent in particles containing heavy (c, b, ...) quarks. For example, the free path of a J/ψ-particle in nuclear matter makes up ~ 10 fm, i.e. the order of the size of heavy nuclei. Therefore, J/ψ particles produced in QGP leave the plasma volume without changing their kinematic characteristics. Experimentally, J/ψ production is identified by the peak in the mass distribution of lepton pairs for the values $M = 3.1$ GeV. As in the case of dilepton production, there of course exists a parton (non-plasma) mechanism of J/ψ production which evidently dominates for not very high energies of colliding hadrons or nuclei. If, however, energies are sufficient for QGP generation and $c\bar{c}$ pairs are produced in the plasma, one should expect an increased yield of J/ψ-particles in events with QGP generation. This was the logic of the pioneering papers [77, 90, 91] investigating heavy-quark-containing particles in QGP. But these papers disregarded the fact $c\bar{c}$-pairs are produced in the medium of light quarks, antiquarks, and gluons at a temperature T. The medium can either strengthen or weaken particle generation processes. Some information on the QCD vacuum at finite temperatures can be gained from QCD perturbation theory [25]. It is well known that for characteristic momenta $p_E \sim g(T) \cdot T$ ($g(T)$ is a QCD "running" coupling constant at finite T) there occurs Debye screening of the chromoelectric component of a gauge field which is quite similar to the electric charge screening in the electron-ion plasma. But there also

exists a new scale $p_M = g^2(T)\,T$ associated with screening of the chromomagnetic component of a gauge field. On the other hand, the QCD vacuum has a much more complicated organization than that presented in perturbation theory. As has already been mentioned, the QCD vacuum properties have been most successfully investigated in the past years in lattice gauge theories (LGT). The screening radius $\xi(T)$ of color charges is calculated in LGT which takes into account not only the theoretical perturbative fluctuations of gauge fields. Obviously, if $\xi(T)$ is smaller than the $c\bar{c}$ bound state radius: $\xi(T) < r_{J/\psi}(T)$ at a given temperature, the production of J/ψ particles in quark-gluon plasma should be expected to be suppressed. The estimates [92] of $r_{J/\psi}(T)$ show that already at temperatures $T \gtrsim 250$ MeV $\xi(T) < r_{J/\psi}(T)$, i.e. the production of J/ψ particles is suppressed. Clearly, the suppression of J/ψ production will affect the character of transverse momentum distribution: screening in QGP causes a decrease of the fraction of J/ψ particles produced with small ($\lesssim 1$ GeV) P_t [93–95].

Recent data of NA 38 Collaboration on the transverse momentum dependence of J/ψ production in ^{16}O-U collisions exhibits the predicted J/ψ suppression at low P_t [96]. But the collisions of produced J/ψ in nuclear matter can give an alternative explanation of the observed effect [97].

Summarizing the presented material on quark-gluon plasma "thermometers", we should note that in spite of lack of knowledge of concrete dynamics of QCP generation and evolution, one may hope to identify quark-gluon plasma signals in the spectra of particles containing heavy quarks and in dileptons in hadron and ion collisions.

3.4. Transverse momentum of hadrons

In the papers [98–100] it was proposed to study the correlation between the transverse momenta and multiplicity with the purpose of identifying the hadron-QGP transition signal. The point is that the dependence of the mean transverse momentum $\langle P_t \rangle$ of secondary particles on hadron multiplicity per unit rapidity dn/dy reflects the hadronic matter equation of state. There exist two mechanisms leading to this relation. When the transverse expansion in the course of hydrodynamic evolution is taken into account, the quantity $\langle P_t \rangle$ turns out to be related to the pressure in the medium [66, 100, 101]. On the other hand, the quantity dn/dy is proportional to the entropy density (or energy density; see, for example, (2.12)). Thus, the degree of increase of $\langle P_t \rangle$ as a function of dn/dy contains information on the equation of state of the medium. In the case of first-order phase transition in the mixed phase the energy density may vary while the pressure remains

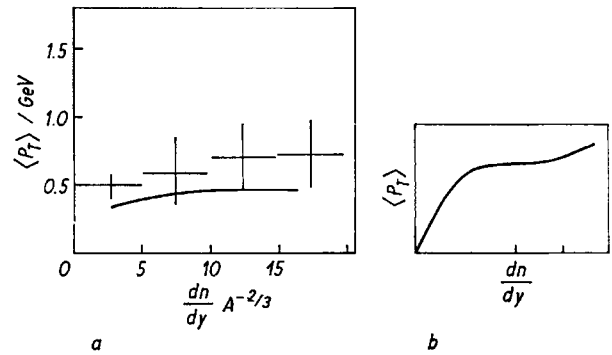

Fig. 18. Mean transverse momentum versus rapidity density (a)-experimental data from UA1 [104] (solid line) and JACEE [106] (crosses), (b)-QGP prediction [100]

constant. This leads to the following qualitative dependence of $\langle P_t \rangle$ on dn/dy (Fig. 18, b [100]). The same dependence results from an account of the contribution from hadron "evaporation" at early stages at $T > T_c$ [103]. It is of interest that such a dependence — an increase of $\langle P_t \rangle$ as a function of dn/dy with a subsequent flattening is observed on $Sp\bar{p}S$-collider [104] (the dashed line in Fig. 18, a) as well as in $p\bar{p}$-interactions on ISR [105] and in cosmic rays [106] (Fig. 18, a). It should be noted that there also exist alternative explanations of this behaviour [107—109].

Conclusion

Can QGP be detected in the already available experimental data? The question is not meaningless because, as has already been mentioned in Sec. 2, the estimates of the parameters of "hadron-QGP" phase transition admit QGP generation on the existing accelerator energies. A paradoxical situation may occur when one is going to seek something that has long before been discovered! This optimistic point of view is based on the agreement of some QGP predictions with experimental data, which was discussed in Sec. 3. But the data presented refer to different experimental techniques and methods and have a different degree of reliability. Therefore it seems too early to declare that QGP has already manifested itself in experiment. On the other hand, it is difficult to imagine that the qualitative coincidence between experimental data and QGP predictions is accidental. The set of QGP generation signals undergoing experimental verification should be as large as possible.

Such experiments are already beeing carried out in two most prominent research centres, CERN and Brookhaven. In CERN, in October 1987 ^{32}S ions were accelerated up to 200 GeV/nucleon. In Brookhaven in 1987 beams of ^{32}S at 15 GeV/nucleon was obtained. The primary goal of these experiments was to discover the new state of the hadron matter — the quark-gluon plasma. Do the ion energies and masses suffice for this purpose? No definite answer to this question can be given at the present time. Experimental plans go even further: in Brookhaven nuclei up to gold (Au^{197}) are planned to accelerate by 1989, and in future to create a heavy ion collider (RHIC) capable of accelerating ions with atomic numbers ~ 200 up to energies ~ 100 GeV/nucleon.

Whether or not the new state of hadron matter — quark-gluon plasma exists can be ascertained only in experiment. Let us hope that the answer will be affirmative.

References

[1] FERMI, E., Progr. Theor. Phys. **5** (1950) 570.
[2] POMERANCHUK, I. YA., Doklady Akad. Nauk. **78** (1951) 889 (in Russian).
[3] LANDAU, L. D., Izvestiya AN SSSR. Ser. Fiz. **17** (1953) 51 (in Russian); Collected Papers of LANDAU, Gordon and Breach, No. 4, 1965.
[4] SAKHAROV, A. D., Soviet. Physics-JETP, Letters **5** (1967) 32.
[5] POLYAKOV, A. M., Phys. Lett. **82 B** (1979) 247.
[6] SUSSKIND, L., Phys. Rev. **D 20** (1979) 2610.
[7] ENGELS, J., et al., Nucl. Phys. **B 205** (1982) 545.
[8] MORLEY, P. D., KISLINGER, M. B., Phys. Rep. **51** (1979) 65.
[9] Proc. Internat. Conf. "Quark Matter '83", Nucl. Phys. **A 418** (1984).
[10] Proc. Internat. Conf. "Quark Matter '84", Springer Lect. Notes in Phys. **221** (1985).
[11] Proc. Internat. Conf. "Quark Matter '86", Nucl. Phys. **A 461** (1986).
[12] Proc. Internat. Conf. "Quark Matter '87", World scientific, Singapore, 1987.
[13] MÜLLER, B., The Physics of Quark-Gluon Plasma, Springer Lect. Notes in Phys. **225** (1985).

[14] Cleymans, I., Gavai, G., Suhonen, J., Quarks and Gluons at High Temperatures and Densities, Phys. Rep. **120** (1986) 217.
[15] McLerran, L., The Quark-Gluon Plasma, Rev. Mod. Phys. **58** (1986) 1021.
[16] Toneev, V. D., Shulz, H., Gudima, K. K., Repke, G., Towards study of hot dense nuclear matter in heavy ion collisions, "Physics of elementary particles and atomic nuclei" **17** (1986) 1096.
[17] Vanyashin, A. V., Emel'yanov, V. M., Nikitin, Yu. P., The Quark-Gluon Plasma (Lectures), MPEI, Moscow, 1987 (in Russian).
[18] Hadronic Matter under Extreme Conditions; Naukova Dumka, Kiev, 1986.
[19] Physics of Many-Particle Systems, 1986, iss. 10 (in Russian).
[20] Chodos, A., et al., Phys. Rev. **D 9** (1974) 3471.
[21] Landau, L. D., Lifshitz, E. M., Statistical Physics, Pergamon Press, 1968.
[22] Gorenshtein, M. I., Zinoviev, G. M., Petrov, V. K., Shelest, V. P., in Ref. [19], p. 3.
[23] Wigner, E., Trans. Faraday Soc. **34** (1938) 678.
[24] Kapusta, J., Nucl. Phys. **B 148** (1979) 461.
[25] Kalashnikov, O. K., Klimov, V. V., Phys. Lett. **88 B** (1979) 328.
[26] Belavin, A. A., Polyakov, A. M., Schwartz, A. S., Tyupkin, Yu. S., Phys. Lett. **59 B** (1975) 85.
[27] Baluni, V., Phys. Lett. **106 B** (1981) 491.
[28] De Corvalho, C. A., Nucl. Phys. **B 183** (1981) 183.
[29] Cross, A. J., Pisarsky, R. D., Yaffe, L. G., Rev. Mod. Phys. **53** (1981) 43.
[30] Shuryak, E. V., Phys. Rep. **67** (1980) 71.
[31] Shuryak, E. V., Phys. Rep. **115** (1984) 153.
[32] Shuryak, E. V., Nucl. Phys. **B 203** (1982) 160.
[33] Polikarpov, M. I., et al., preprint ITEP-160, 1986.
[34] Shuryak, E. V., Phys. Lett. **107 B** (1981) 103.
[35] Levin, E. M., Frankfurt, L. L., Soviet. Physics-JETP, Letters **2** (1965) 106.
[36] Shuryak, E. V., Phys. Lett. **79 B** (1978) 135.
[37] Shifman, M. A., Vainshtein, A. I., Zakharov, V. I., Nucl., Phys. **B 147** (1979) 385; **448**, 519.
[38] Bochkarev, A. I., Shaposhnikov, M. E., Soviet Physics-JETP, Letters **39** (1984) 488.
[39] Bochkarev, A. I., Shaposhnikov, M. E., Nucl. Phys. **B 268** (1986) 220.
[40] Pisarsky, R. D., Phys. Lett. **110 B** (1982) 155.
[41] Wilson, K., Phys. Rev. **D 10** (1974) 2445.
[42] Engels, J., Karsch, F., Montvay, I., Satz, H., Phys. Letters **101 B** (1981) 89; **102 B**, 332.
[43] Engels, J., Karsch, F., Satz, H., Nucl. Phys. **B 205** (1982) 239.
[44] Karsch, F., Nucl. Phys. **B 205** (1982) 285.
[45] McLerran, L., Svetitsky, B., Phys. Rev. **D 24** (1981) 450.
[46] Kajantie, K., et al., Z. Phys. **C 9**, (1981) 253.
[47] Çelik, T., et al., Phys. Lett. **B 125**, (1983) 411.
[48] Çelik, T., et al., Phys. Lett. **B 129** (1983) 323.
[49] Banks, T., Ukawa, A., Nucl. Phys. **B 225**, (1983) 145.
[50] Shuryak, E. V., Nucl. Phys. **B 203** (1982) 93; 114; 140; **B 124** (1983) 237.
[51] Engels, J., et al., Preprint BI-TP 82/08.
[52] Engels, J., et al., Phys. Lett. **B 102** (1981) 332.
[53] Černý, V., Lichard, P., Pišút, J., Phys. Rev. **D 16** (1977) 2822; **D 18** (1978) 2409; **D 20** (1979) 699.
[54] Kajantie, K., Matsui, T.,Phys. Lett. **164 B** (1985) 373.
[55] Baym, G., Phys. Lett. **138 B** (1984) 18.
[56] Bjorken, J. D., Weisberg, H., Phys. Rev. **13** (1976) 1405.
[57] Sumiyoshy, H., et al., Z. Phys. **C 23** (1984) 391.
[58] Van Hove, L., Z. Phys. **C 21** (1983) 93.
[59] Bjorken, J. D., Phys. Rev. **D 27** (1983) 140.
[60] Hwa, R. C., Kajantie, K., Phys. Rev. Lett. **56** (1986) 696.
[61] Carruthers, P., Los Alamos preprint LAUR-85-280.
[62] Zhirov, O. V., Sov. J. Nucl. Phys. **30** (1979) 1098.
[63] Hwa, R. C., Phys. Rev. **D 10** (1974) 2260.
[64] Chiu, C. B., Sudarshen, E. C., Wang, K. H., Phys. Rev. **D 12** (1975) 902.
[65] Zinoviev, G. M., Pavlenko, O. P., Shelest, V. P., in Ref. [19], p. 65.

[66] Milekhin, G. A., Proc. Internat. Cosmic Ray Conf., Moscow, 1959, v. 1, p. 220.
[67] Anishetty, R., Koehler, P., McLerran, L., Phys. Rev. **D 22** (1980) 2793.
[68] Kajantie, K., McLerran, L., Phys. Lett. **119 B** (1982) 203.
[69] Hwa, R. C., Kajantie, K., Phys. Rev. **D 32** (1985) 1109.
[70] McLerran, L. D., Toimela, T., Phys. Rev. **D 31** (1985) 545.
[71] Manielewicz, P., Guilassy, M., Phys. Rev. **D 31** (1985) 53.
[72] Hosoya, A., Sakagami, M., Takao, M., Ann. Phys. (NY), **154** (1984) 229.
[73] Chu, M. C., Phys. Rev. **D 34** (1986) 2764.
[74] Feinberg, E. L., in Proc. Kiev Conf. in High Energy Physics, 1959, v. 2.
[75] Domokos, G., Goldman, J. I., Phys. Rev. **D 23** (1981) 203.
[76] Kajantie, K., et al., Phys. Rev. **D 34** (1986) 2746.
[77] Shuryak, E. V., Phys. Lett. **78 B** (1978) 150; Sov. J. Nucl. Phys. **28** (1978) 408.
[78] Specht, H. J., in Ref. [10], p. 221.
[79] Voloshin, S. A., Nikitin, Yu. P., in "Elementary Particles and Atomic Nucleus", Energoatomizdat, Moscow, 1986, p. 3 (in Russian).
[80] Emel'yanov, V. M., Nikitin, Yu. P., Preprint MPEI No. 061—86, Moscow, 1987 (in Russian).
[81] Faessler, M. A., preprint CERN-EP/86-102.
[82] Michael, C., Phys. Lett. **63 B** (1976) 301.
[83] Haber, B., et al., Phys. Rev. **D 22** (1980) 2107.
[84] Andersson, K. J., et al., Phys. Rev. Lett. **36** (1976) 237.
[85] Blokus, D., et al., Nucl. Phys. **B 201** (1982) 205.
[86] Gorenstein, M. I., Pavlenko, O. P., preprint ITP-87-3E, Kiev, 1987.
[87] Willis, W. J., in Proc. Uppsala conf., 1987.
[88] Černý, V., Lichard, P., Pišýt, J., Z. Phys. **C 31** (1986) 163.
[89] Von Gersdorff, H., et al., Phys. Rev. **D 34** (1986) 794; 2763.
[90] Cleymans, J., Philippe, R., Z. Phys. **C 22** (1984) 271.
[91] Reusch, H. J., Z. Phys. **C 26** (1984) 105.
[92] Matsui, T., Satz, H., Phys. Lett. **178 B** (1986) 416.
[93] Karsch, F., Petronzio, R., Phys. Lett. **193 B** (1987) 105.
[94] Vanayashin, A. V., Emel'yanov, V. M., Soviet Physics-JETP, Letters, **45** (1987) 513.
[95] Ruuskanen, P. V., Satz, M., Preprint BNL-40438, 1987.
[96] Abreu, M. C., et al., Preprint CERN-EP/88-25, 1988.
[97] Ftačnik, J., Lichard, P., Pišút, J., Comenius Univ. preprint, Bratislava, 1987.
[98] Shuryak, E. V., Zhirov, O. V., Sov. J. Nucl. Phys. **28** (1978) 485.
[99] Shuryak, E. V., Zhirov, O. V., Phys. Lett. **89 B** (1980) 253.
[100] Van Hove, L., Phys. Lett. **118 B** (1982) 138.
[101] Kataja, M., et al., Phys. Rev. **D 34** (1986) 2755.
[102] Gorenstein, M., Pavlenko, O., Zinovjev, G., Preprint ITP 74-95 E, Kiev, 1974.
[103] Zinovjev, G., Gorenstein, M., Pavlenko, O., Nucl. Phys. **B 252** (1985) 197.
[104] Arnison, G., et al., Phys. Lett. **118 B** (1982) 167.
[105] Breakstone, A., et al., Phys. Lett. **183 B** (1987) 227.
[106] Burnett, T. H., et al., Phys. Rev. Lett. **57** (1986) 3249.
[107] Capella, A., Pajares, C., Ramallo, A. V., Nucl. Phys. **B 241** (1985) 75.
[108] Barshay, S., Phys. Rev. **D 29** (1984) 1010.
[109] Bopp, F. W., et al., Phys. Rev. **D 33** (1986) 1867.